RADAR TARGET DETECTION AND CLASSIFICATION USING WAVELET SCATTERING AND NEURAL NETWORK

A THESIS SUBMITTED TO
THE FACULTY OF ARCHITECTURE AND ENGINEERING
OF
EPOKA UNIVERSITY

BY

ERINDA BRAHO

IN PARTIAL FULFILLMENT OF THE REQUIREMENTS
FOR
THE DEGREE OF MASTER OF SCIENCE
IN
ELECTRONICS AND COMMUNICATIONS ENGINEERING

JULY, 2021

Approval sheet of the Thesis

This is to certify that we have read this thesis entitled **“**Radar Target Detection and Classification Using Wavelet Scattering And Neural Network**”** and that in our opinion it is fully adequate, in scope and quality, as a thesis for the degree of Master of Science.

____

Dr. Arban UKA
Head of Department
Date: _________________

Examining Committee Members:

Dr. Arban UKA	(Computer Engineering)	__________________
Dr. Julian HOXHA	(Computer Engineering)	__________________
Dr. Shkëlqim HAJRULLA	(Computer Engineering)	__________________

I hereby declare that all information in this document has been obtained and presented in accordance with academic rules and ethical conduct. I also declare that, as required by these rules and conduct, I have fully cited and referenced all material and results that are not original to this work.

Name Surname: Erinda Braho

Signature: _______________

ABSTRACT

RADAR TARGET DETECTION AND CLASSIFICATION USING WAVELET SCATTERING AND NEURAL NETWORK

Braho, Erinda
M.Sc., Department of Electronics and Communications Engineering
Supervisor: Dr. Julian Hoxha

Radars are used in a variety of environments, and their main purpose is to achieve the correct target detection. One of the most important research issues and technologies in modern radar is moving target classification and identification using radar echoes. This study has explained the theory of radar and usage of wavelet scattering and backscattering to classify a target. A short introduction for neural network and Long Short-Term Memory is explained and what is their contribution in classification and reduction of time required to complete the radar target detection.

Keywords: *Wavelet scattering, radar, target classification, radar cross section, wavelet transform, radar response*

ABSTRAKT

IDENTIFIKIMI DHE KLASIFIKIMI I OBJEKTEVE NEPERMJET RADARIT, DUKE PERDORUR SHPERNDARJEN E VALEVE DHE RRJETIN NEURAL

(Leave one empty line)

Braho, Erinda

Master Shkencor, Departamenti i Inxhinierisë Elektronike dhe te komunikimit

Udhëheqësi: Dr. Julian Hoxha

Radarët përdoren në një larmi ambientesh dhe qëllimi i tyre kryesor është të arrijnë identifikimin e saktë të një objekti. Një nga çështjet kryesore në punimet shkencore është identifikimi I një objekti në lëvizje, duke perdorur jehonën e valëve. Ky studim ka shpjeguar teorinë e radarit dhe përdorimin e shpërndarjes së valëve dhe kthimit mbrapsht të tyre, për të klasifikuar një objektiv. Si fillim ështe prezantuar një hyrje e shkurtër për përdorimin e rrjetit Neural dhe LTSM, si dhe cili është kontributi i tyre në klasifikimin dhe zvogëlimin e kohës së nevojshme për të përfunduar identifikimin e synuar të objektit nga radari.

Fjalët kyçe: *Shpërndarja e valëve, radari, identifikimi I objektivit, ndër seksioni I radarit, transformimi i valëvet, përgjigja e radarit*

Dedicated to my parents, Kamber & Flutura Braho

ACKNOWLEDGEMENTS

Throughout my journey at Epoka University, I have received a massive support and assistance from all the professors.

I would first like to thank my supervisor Professor DR. Julian Hoxha, whose support was very valuable during all the research. I want to thank you for your patient support and for all of the opportunities I was given to complete my research and also for counseling me during all my study years here at Epoka University. You have been very supportive and a true role model for all your students.

I owe a deep sense of gratitude to Prof. DR. Betim Çiço for his dedication and keen interest to help all his students including me, in order to achieve the perfect knowledge for doing a research, by providing us with guides for our framework.

I am deeply grateful to Head of Department also my professor DR. Arban Uka whose help was invaluable in particular for me, during these difficult times of a pandemic. His support made it easy for us to achieve our goals and also to successfully accomplish the academic year.

Thanks, and appreciation are extended to every member of the University, for the lecturers who were passionate and careful with us and steered us to the right direction.

Finally, I want to thank my family, friends and colleagues, who in one way or another shared their support, either morally, financially or physically.

Table of Contents

LIST OF FIGURES

CHAPTER 1

INTRODUCTION

1.1 Problem Statement

Radar Application is one of the most intriguing field of study for us as Electronics Engineers. With all of the technology advances happening in today’s world, using of the Radars to have machine to machine communication, without human interference is fascinating. One of the main usage of radars is in aviation industry which is evolving fast, and during the flight every communication happening with the Control Tower, occurs using these radar impulses. Considering the benefits that we get from aviation and radar application; it would be good to perform this research in order to distinguish possible shortcomings and maybe accomplish initiatives to make new advances.

Radar, which stands for radio detection and ranging, is a sort of instrument that is used to detect, localize, track, and characterize objects in a limited environment. The mechanism of operation is based on measuring the time of flight and energy of transmitted sets of pulses dispersed off from targets in a field of view. A target is present if the received echo has enough power to distinguish itself from noise, clutter, or interference. The distance to the target can be calculated by monitoring the duration between transmission and reception. The horizontal and vertical angles to the target can be determined using a scanning system or several transmitters or receivers. Target signatures (such as micro-motions) can be utilized to characterize (classify) the target if the system has suitable resolution. Multiple targets can be recognized, located, and described simultaneously if the system's measurements have few ambiguities. Each target can be tracked over a series of frames using several target tracking algorithms. As a result, radar systems are extremely capable, giving all necessary data for establishing a complete situational awareness of monitored areas.

Our research studies target detection of radar, the signals contained in radar systems are discussed, as well as how the information they provide about targets might be employed for fusing. Radar Cross Section characterizes every radar. “Radar Cross Section is a measure of a target's capacity to backscatter incident energy to radar, and it is typically related to the target's geometrical complexity. This radiated energy enables for the acquisition of many important places on the target, which are referred to as scattering centers. It is generally known that these centers are capable of accurately describing a target.” [1]

This research discusses the problem of radar target recognition based on RCS, and wavelet scattering. “The scattering mechanisms in radar systems that describe the behavior of objects in response to incident waves can be divided into two categories: dispersive and non-dispersive scattering mechanisms. The local scattering features can be recovered from the local maxima of the target response in the time domain for non-dispersive scattering such as corners, edges, or specular reflections.” [2]

1.2 **Thesis Objective**

In this thesis, will be introduced basic concepts for radars, radar equation and radar cross section. The purpose is for the reader to create the idea on how the radars work, what is their purpose and of course to meet the goal of this research, how to classify radar targets.

Later in this research we are presenting wavelets, and its transform also Continuous and Discrete Wavelet Transforms. Objects are classified based on what wavelet is applied to them and application of wavelets in RCS is presented. The main objective of these short explanations done in chapter 3, is to examine how radar targets behave and what is the best way to classify them.

1.3 Scope of Work

In order to meet the objective of this research, we have conducted an analytical research, by which we have taken one already solved MATLAB example [3] and made the necessary modifications to see how the output would be and to help us achieve Radar Target Classification.

1.4 Organization of the thesis

Our research is divided in 5 Chapters. The organization is done as follows: Chapter 1 states the problem, gives the objective of the thesis and scope of work is presented. Chapter 2 includes the Literature Review done for this research. In Chapter 3 we have discussed in detail what is radar, how does radar work? Also, we have explained the main key words of wavelet scattering, application of wavelets in RCS, Radar Cross Section and Simulation based on some of the papers discussed in Chapter 2. Chapter 4 includes our methodology and experiments. While Chapter 5 has conclusions and future work.

CHAPTER 2

LITERATURE REVIEW

As previously mentioned, this research studies radars, wavelet scattering and radar cross section. In order to have a basic idea how these are connected and achieve Radar target classification 50 papers were considered and different books and studies to review each subject individually and then to make the connection between them and how they accomplish our goal for this thesis.

“The transformed image in the range-scale domain is obtained by applying wavelet principles to stepped frequency backscattered data reflected from nondispersive scattering centers of an object in this research” [4] . In radar systems, each frequency component can be analyzed for the extraction of object behavior to the incident high frequency wave with a resolution equal to its scale. To create multiresolution range profiles, the processing splits the modified image into numerous slices along the scale axis. “A local modulus maxima algorithm, which shows the scattering distribution over the radial distance in the range-domain, parameterizes information about scattering centers in terms of scales and local peaks. For the local maxima extraction, various multiresolution range profiles are used to acquire trustworthy positions of the scattering centers. The coincident method is then used to pinpoint the exact location of the suitable scattering centers. The significant range profile can be used to generate feature vector sets that can be used for automatic target detection or target signature storage in the wideband stepped frequency radar.” [4]

The findings on paper [5] suggest that any ground target passing or entering its coverage area is detected and classified using a micro-sensor network system of Forward Scattering Radar (FSR). The system's efficiency is determined by its classification performance, which is strongly dependent on the data collected from the signal. As a result, it is crucial to pick the right transformation strategies for extracting the required information from the target signal. The Wavelet Technique (WT) is utilized in this paper to provide scales and variation information. This data will be taken and used as part of the classification process. The wavelet technique is used to display the similarity of signals from distinct targets and the dissimilarity of signals from distinct targets.

Paper [6] considers synthetic aperture radar and its approach on detecting which is based on image application. Due to the complicated imaging mechanism of SAR imaging, SAR images have a low signal to noise ratio, posing significant obstacles and difficulties in target detection. As a result, increasing the SNR, or the difference between the gray value of the target and the background area, is the most important step in enhancing the target detection rate of SAR images. In SAR images, the coherent imaging technique generates high amount of speckle noise, which has considerable impact on target detection. This work developed the SWT-BEMD algorithm, a new SAR image target detection approach based on the two-dimensional stationary wavelet transform (SWT) and bidimensional empirical mode decomposition, to reduce speckle noise and increase SNR (BEMD). After the image was decomposed by BEMD, certain bidimensional intrinsic mode function (BIMF) feature components were recovered, allowing for the expansion of gray difference between target and background. The SWT-BEMD method enhances target identification rates, particularly for small, hidden, and weak scattering objects, while also reducing the impact of speckle noise and background clutter. The SWT-BEMD algorithm's performance was verified using SAR image data, and the experimental findings suggest that it is both effective and practicable.

Another approach on noise-based wavelet transforms in the received Ultra-Wideband pulse is analyzed on paper [7]. The impulse shape and position can be determined from the transform results using an analytical version of the wavelet. By using thresholding technology to deal with the coefficients, the impulse samples may be recreated, and noise reduction can be achieved. The echo time delay of scattered target components might be approximated in order to speed up the range profile processing of UWB radar.

Paper [8] is presented on 1995 in an IEEE conference and it interprets scattering mechanism of Radar Target by using wavelet transform. “Target identification relies heavily on the locations, scattering strength, and scattering mechanism of the centers. By studying local frequency components of radar ranges, this work proposes a method for determining the placements, scattering strengths, and scattering mechanisms of these scattering centers."

Zh. Sebbani and Delisle have studied Radar Cross Section Decomposition and Wavelet scattering on paper [9] and paper [10]. Both these studies were presented on IEEE conferences in 2005. They saw that it was a promising approach in order to achieve a high-level identification of the complex target if the wavelet signal processing could identify RCS. The technique of decomposition was applied on RCS sample target and then on complex targets. The RCS ranges that are properties of the geometrical properties of the objects are provided by the decomposition. To increase recognition performance in far-field circumstances, the proposed methodology was applied to simple and complex targets. The method is most suited for analyzing scatters with difficult-to-interpret RCS, and the findings yield good recognition and identification outcomes. Because it has no fundamental limitations, the technology might be applied to a variety of tough near-field identification problems.

The radar target prediction study [11] discusses the use of a Forward Scattering Radar to detect ground targets (FSR). In this paper, the topic of obtaining the Doppler signature in various interference settings is discussed. The target's existence was predicted using Hilbert Transform and Wavelet. The paper starts with a basic overview of the system, then moves on to a more in-depth analysis of predicting the presence of a target in Forward Scattering Radar.

The work done on paper [12] which we also referred on our chapter 3, is an analysis done on four different techniques which are applied on Short Fourier Transform, Adaptive Wavelet Transform, Evolutionary Adaptive Wavelet Transform and Continuous Wavelet Transform. Scattering centers and resonance frequencies are two scattering phenomena that are crucial for radar target signature analysis. The similarities of four alternative time-frequency evaluation techniques are provided in the simulation using wire target data. The results demonstrate that the EAWT is the most effective method for simultaneously analyzing scattering centers and resonance frequency.

Paper [13] investigates ultra-wide band (UWB) applications, a unique triangular patch antenna with reduced RCS is proposed. The goal of antenna innovation is to achieve Reduced Radar Cross Section. The patch was slid into place and techniques of reduction are employed. To improve RCS, a radiating patch is invented, with two slots notched on it to retain good radioactivity performance and increase impedance matching of the planned antenna. The Radar Cross Section function of a new antenna is evaluated and compared to a reference patch. The new patch has an improved RCS in practically all of the operational frequencies of 2-12GHz, from this we see that gain is satisfactory in the wide band frequency. The simulation done in this paper shows that the designed antenna has a good potential for antenna applications of low Radar Cross Section.

The method used on paper [14] is an Empirical Wavelet Transform which extracts scattering centers for target identification. The EWT is used to extract scattering centers for targets whose radar returns are collected using a stepped frequency method, which are subsequently used for target identification. The method is first validated using synthetic target models before being used to real radar backscatter from commercial aircraft models captured in the upper resonance area.

Shadow image of bistatic forward scattering radar, an improved joint time frequency technique was used and assessed (BFSC) is presented on [15]. The revised joint time frequency technique is proven to be an effective and reliable way for removing ground clutter and direct signal for BFSC shadow imaging, which are two critical elements that affect image quality.

[16] discusses scattering behavior of multi layered dielectric and magnetic barriers which is a difficult topic with lots of applications. The bistatic RCS of 2-D scatters made up of lossy magnetic and insulator materials, such as Perfect Conductor Metals, is calculated using a surface formulation, the method of Moments (MoM), and a wavelet-like matrix in this paper.

RCS of a radar target is commonly defined as a function of the number of significant scattering spots. These scattering locations, however, are insufficient to estimate the target's size. When wavelet pyramidal decomposition is used to the RCS interpretation, improves the amount of information consequently leading to better results

This is the central finding of this paper. This paper dates back to 1999 and explains wavelet pyramidal decomposition also what its usage on RCS is. [17]

“The information of the flying attitude is contained in the amplitude envelope of monochromatic Doppler radar echo for the projectile with slots at the bottom on paper” [18]. The echo can be described as an amplitude modulation and frequency modulation signal due to the projectile's nonlinear movement. “A hybrid approach based on the Teager energy operator and wavelet transform is suggested to extract the envelope of radar echo dispersed by the slotted projectile and successfully separate the amplitude from frequency modulation. The echo model was first defined, and its characteristics were briefly discussed. The Teager nonlinear energy-tracking operator was then introduced to the echo and applied. The noise, however, severely distorted the envelope obtained. The noise was then suppressed using the stationary wavelet transform. The hybrid technique's efficiency is demonstrated by a comparison of the denoised envelope, and the radar cross section recorded in the static state.”

Using the Numerical Electromagnetics Code and measurements from a High Frequency Surface Wave Radar system in Cape Race, Newfoundland, Canada, the radar cross sections (RCS) of both small and large ships for High Frequency Surface Wave Radar were investigated on paper [19]. “This study was conducted using radars for ships and cargos and made an experiment by comparing Teleost signals to reflections from seven cargo-container ships discovered during the HFSWR's operational evaluation. The study concludes that Teleost and big cargo-container vessels have an angle-averaged RCS of -40dBm2, whereas small vessels (under 1000 tons) could reasonably be described by an angle-averaged RCS of -30 dBm2, in the lower frequency range.”

The Radar Cross Section is always used to identify a radar target (RCS). However, scattering points are insufficient to estimate the dimension of Radar targets, thus a solution to this problem appears to be required. “Normally, the characteristic space is decomposed using Wavelet pyramidal decomposition to retrieve information about the target's size. The recognition of a complex target is the subject of research” [1].

Another concept for Radar Cross Section is discussed on paper [20]. “If the RCS of a target is measured in a non-Faraday cage measurement facility, the RCS of the target may be contaminated by outside transmissions in the same spectral band as the measurement. Outside radiations will pollute the value of the measured RCS in this case, and as a result, their level must be decreased in order to obtain accurate RCS measurements.” The use of wavelets in this article is used to provide a mathematical strategy for reducing the effects of interferences on RCS measured values. The use of wavelets in this article is used to provide a mathematical strategy for reducing the effects of interferences on RCS measured values.

“The arbitrarily dimensional rapid lifting wavelet-like transform is used to achieve the Asymptotic Waveform Evaluation methodology in the” [21] research. The sparse matrix equation in the wavelet domain is first constructed using the novel preprocessing methodology. The AWE methodology is used to obtain the wide band solution of this sparse linear system, an inverse wavelet transform is used to calculate the real induced surface current. The efficacy of the present method has been demonstrated by numerical modeling of variously shaped three-dimensional objects.

On paper [22] “the following three average radar cross sections (RCS) for any target at any aspect angle have been proven in this paper: satisfy a simple proportional relation, i.e., 3: 2: 1 for polarization matched radar, common antenna radar, and cross polarization radar. Assume that the radar transmitting polarization runs on the Poincaré system, and that the average is the probability average, with uniformly distributed probability of the density function.”

One of the most referred paper on our research is paper [23]. This study proposes a method “to decompose maneuvering target RCS into RCS of a specific pose and RCS of a random pose, taking into account that maneuvering target RCS fluctuates with the target's posture acutely”. The RCS of a particular pose is sensitive to changes in the moving goal pose, and it is strongly dependent on the pose. “Then the Radar Cross Section of random pose is passed as noise. The paper employs wavelet analysis to process maneuvering target RCS sequences with wavelet analysis based on the characteristic De-noising. We can get the RCS sequence of De-noising changed with posture using this way (RCS sequence of certain pose).”

Studying radar and multifunctional radar we have variety of signals, paper [24] analyzes this. Because of its high performance, multifunction radar has been widely used. The multifunction radar, on the other hand, can detect a wide range of signal kinds. The most perplexing part of environmental cognition is how to recognize multifunction radar. This work provides a wavelet-based signal cognition system for analyzing and estimating signal modulation types in complex electrical data. “A micro-Doppler moving feature model was constructed based on target moving characteristics and electromagnetism scattering theory, which disclosed the features of amount, geometry center location, and sliding phenomenon. The proposed method may effectively increase the performance of radar environment cognition and make target recognition more feasible, according to experimental results.” [24]

The utility of wavelet expansions in linearized inverse scattering situations is demonstrated in [25]. We motivate the usage of wavelet expansions in this communication and prove their utility in the non-linearized case using numerical examples. There are two alternative techniques to multiresolution, which we call fixed and dynamic multiresolution, respectively.

CHAPTER 3
THEORY OF RADAR

3.1 Radar

The terms "radio tracking and ranging" are combined to form the term "radar." The original aim of a radar was to use radio waves to identify the presence of a target and determine its scope. Radars today are capable of not only detecting targets and measuring distances, but also of finding, imaging, and recognizing them. “A transmitter, an antenna, a receiver, a signal processor, and a monitor are all part of a typical radar.” [26] Radars come in a variety of shapes and sizes. Monostatic radars and bistatic radars are categorized based on the physical relationship between the antennas that receive signal and transmitting. Radars are known as either continuous wave radars or pulsed radars based on the waveforms they transmit. The ACW radar's transmitter is still on. Pulsed radar sends out a short spurt of pulses, with the receiver turning on after each pulse to receive the echo. Radars are divided into two types based on their primary missions: search radars and tracking radars. Search radars constantly search a large area without settling in one spot. “Their primary missions are to detect targets and determine the range and direction of those targets. Individual targets are tracked by tracking radars in terms of range, azimuth, elevation, and/or Doppler.” [26]

3.1.1 Equation of Radar

“The range of a radar is related to the transmitter, receiver, antenna, target, and distance using a radar equation. Take, for example, a monostatic radar. Pt is the transmitted power, G is the antenna gain, and R is the target distance.” [26, pp. 671-690] The power density at the goal is then calculated as follows:

$$P_d = \frac{P_t G}{4\pi R^2} \tag{1}$$

“Assume the target receives incident power with a region σ, known as the radar cross section (RCS), and radiates in an isotropic manner. As a result, the power density at the radar is:

$$P_d' = \frac{P_d \sigma}{4\pi R^2} = \frac{P_I G_r \sigma}{(4\pi R^2)^2} \tag{2}$$

Assume the radar antenna has an effective area A_e, which is related to the antenna gain by $A_e = G_r\lambda^2/4\pi$.” [26] Then, the power received by the radar is as written here:

$$P_r = P_d A_e = \frac{P_t \cdot G_t \sigma G_r \lambda^2}{(4\pi R^2)^2 \cdot 4\pi} = \frac{P_t G^2 \sigma \lambda^2}{(4\pi)^3 R^4} \tag{3}$$

Where transmitting and receiving data, the same antenna is used. Let S_{min} denote the smallest signal which can be detected, and let RCS σ denote the max range over which a target can be found:

$$R_{max} = \left[\frac{P_t G^2 \sigma \lambda^2}{(4\pi)^3 S_{min}}\right]^{1/4} \tag{4}$$

3.1.2 Radar Cross Section

The equivalent area of a target which is seen by a radar is called Radar Cross Section (RCS) as it is seen on Figure 1. It is the fictitious region that intercepts the sum of power that, when it is scattered evenly in all the directions, generates a radar echo equal to the targets. In mathematical terms it is written in the formula below:

$$\sigma = \lim_{R\to\infty} 4\pi R^2 \frac{|E_s|^2}{|E_i|^2} \tag{5}$$

“Where:

•R = distance between radar and target

•Es = scattered field strength at radar

•Ei = incident field strength at target” [27]

“The Radar Cross Section is a measurement of the Radar target's capacity to scatter irradiation Hertzian waves. The target RCS can be retrieved by radar during the target detection phase, and it is useful information for all system radars. The physical structure of the target, the frequency of radar Hertzian waves, the polarization mode of the incidence field, the polarization mode of the receiving antenna, and the target posture are usually the factors that determine the target RCS.” [27] [28] The RCS can be seen of as a function in mathematics; however, it is a complicated function. It cannot be used to figure

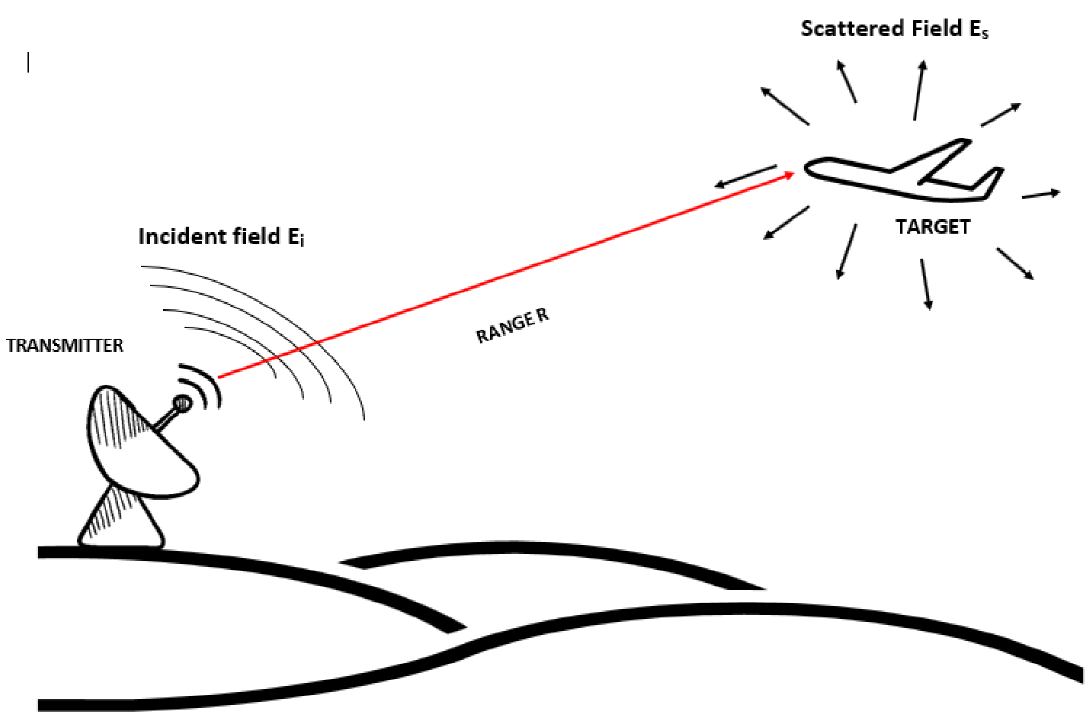

Figure 1 Definition of Radar Cross Section

out a more precise physical structure. The RCS frequently undulates when the goal pose is used. The RCS can shift by several decades dB when the posture angle varies by several degrees. And this is when the RCS comes into play.

The radar targets are usually moving. We create a maneuvering target track that is made up of two parts: a specific maneuvering target path and a random maneuvering target wave. As a result, the target RCS involve both specific and random RCS. The random Radar Cross Section, on the other hand, can be considered a noise sequence. The foundation of Radar data processing is the decomposition of the target RCS.[20] In mathematics, a wavelet is referred to as a microscope. Because it is based on frequency and time, it may effectively minimize noise. This study examines the moving target RCS and first establishes a mathematical model, then uses the wavelet to deconstruct the RCS. It has a better effect.

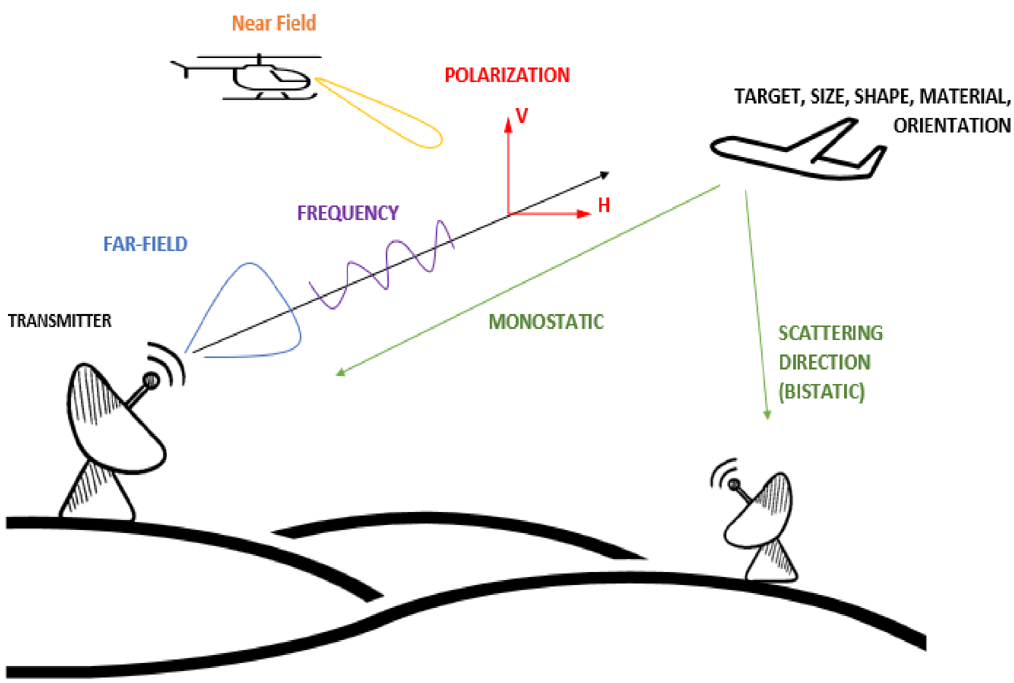

Figure 2 Factors that Determine RCS.

3.1.3 RCS Target Model

"This modeling target is based on [23]. We name the target structure S, Hertzian waves frequency is f, the polarization of incidence field is H_i and H_s is the polarization mode of receiving antenna while the target pose is θ^T. RCS can be expressed as :" [28]

$$RCS=\sigma\,(S, f, H_i, H_T, \theta^T) \tag{6}$$

"In equation 6, the target structure S is certain, and the Hertzian waves frequency f, the polarization mode of the incidence field H_i, and the polarization mode of the receiving antenna H_s are all determined by the certain radar. As a result, target pose θ^T is the main factor, and RCS can be expressed as :" [28] [29] [2] [5] [30] [7]

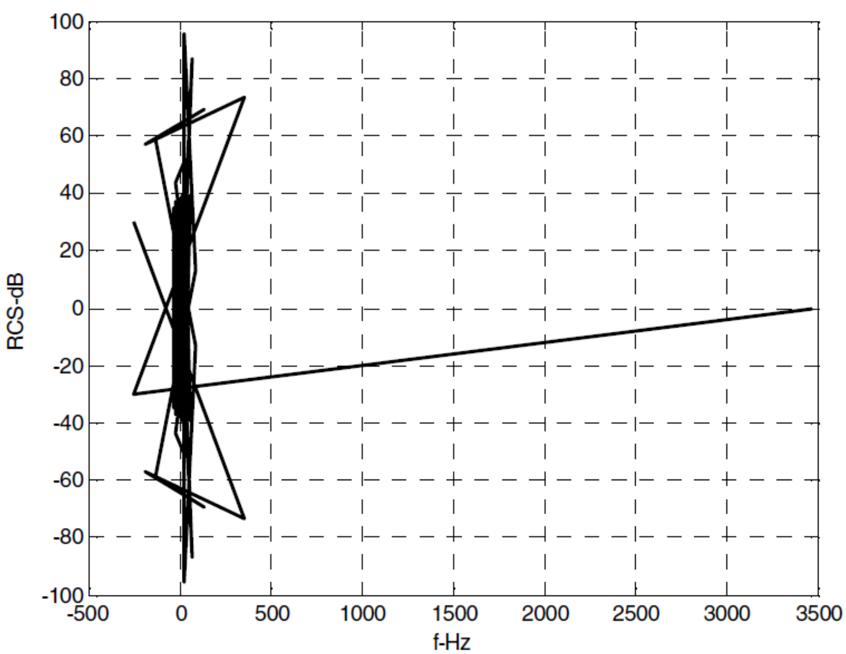

Figure 3 RCS Sequence mixed in frequency. *[28]*

$$\mathrm{RCS}=\sigma(\theta^T) \tag{7}$$

"In the figure 4 it is presented a target RCS contour with azimuth (0-360º) and pitching (0-360º). The target attitude changes over time for the maneuvering target. It can also be thought of as a combination of a specific pose and a random pose. A specific pose is determined by a certain track in the target movement process, but a random pose is determined by the atmosphere disturbing and wobbling. If we study the relationship between RCS and azimuth, the azimuth is θ and the certain azimuth would be φ, random azimuth is Δφ. Formula (8) than would become:" [28]

$$\mathrm{RCS} = \sigma\,(\varphi + \Delta\varphi) \qquad (8)$$

The target is also considered as optics target. This means that radar Hertizian wave lengths are smaller in size than target. From this the RCS is written

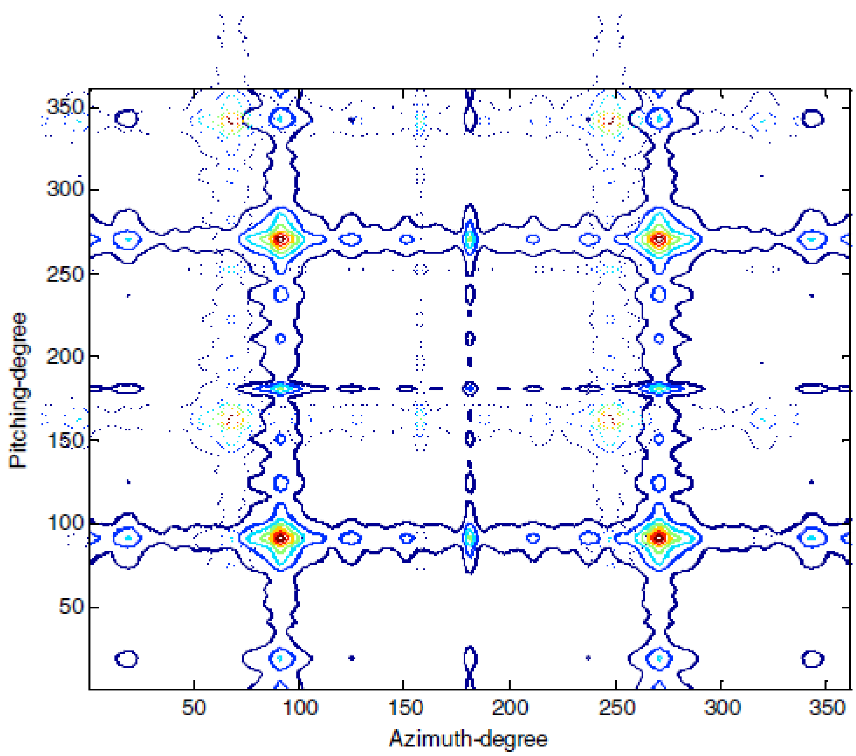

Figure 4 A target RCS *[28]*

$$\sigma(\varphi + \Delta\varphi) = \sum_{i=1}^{n} \sum_{j=1}^{n} \sqrt{\sigma_i \cdot \sigma_j} \cos\left(2k \cdot \left(R_i - R_j\right) \cdot \cos\left(\varphi + \Delta\varphi\right)\right) = \sum_{i=1}^{n} \sum_{j=1}^{n} \sqrt{\sigma_i \cdot \sigma_j} \cos\left\{2k \cdot \left(R_1 - R_j\right) \cdot [\cos(\varphi) \cdot \cos(\Delta\varphi) - \sin(\varphi) \cdot \sin(\Delta\varphi \right. \quad (9)$$

R_i would be the distance between radar and the i-scattering center, σ_i is RCS i-th scattering center. $\Delta\varphi$ is considered noise:

$$\text{Cos}(\Delta\varphi)=1 \quad \sin(\Delta\varphi)=\Delta\varphi \quad (10)$$

From equation 10 we describe equation 9 as

$$\sigma(\varphi + \Delta\varphi)=\text{g}(\varphi)+\text{w}(\varphi, \Delta\varphi) \quad (11)$$

"Where g (φ) is the target certain RCS as previously mentioned, determined by a certain pose. w ($\varphi, \Delta\varphi$) is RCS determined by the certain and random pose and it is a two dismension function.
The random pose can be thought of as the random asway value in the adjacent field of a specific pose. In fact, we consider the random pose to be caused by the atmosphere and target shaking when we describe it. It means that different poses have distinct random wobbles. Equation (11), on the other hand, can be stated as

$$\sigma(\phi + \Delta\phi) = g(\phi) + w(\Delta\phi) \quad (12)$$

The aspect angle has a significant impact on the RCS of a complex target that is massive in comparison to a wavelength. The RCS can fluctuate by several tens of decibels with a slight shift in the aspect angle. Where the equation shows that the target RCS sequence can be composed by certain RCS sequence and random RCS sequence. This is the precondition." [28]

3.1.4 RCS Target Model Simulation

"The simulation is used to validate the strategy using MATLAB's wavelet toolbox. The original RCS sequence is referred to as an unprocessed noise RCS sequence. The filtering noise RCS sequence is also regarded as a specific pose RCS sequence [5]. When you subtract the original RCS sequence from the particular pose RCS sequence, you get the random posture RCS sequence. The wavelet functions are 'Daubechies2' and 'wbmpen'. The decomposition level is 5, alpha the threshold value is 2." [28]

This stimulation it is shown on the figures below:

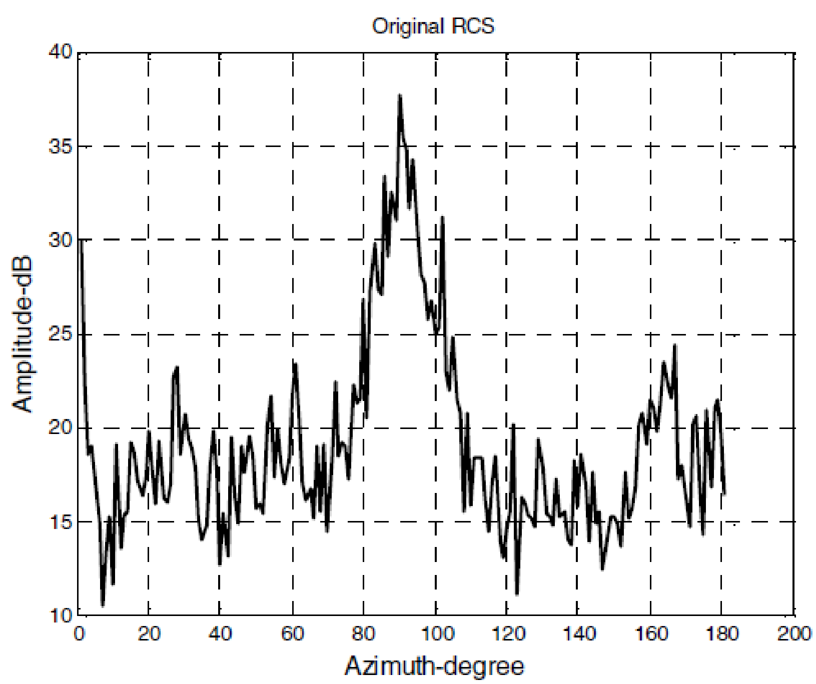

Figure 5 a target original RCS curve *[23]*

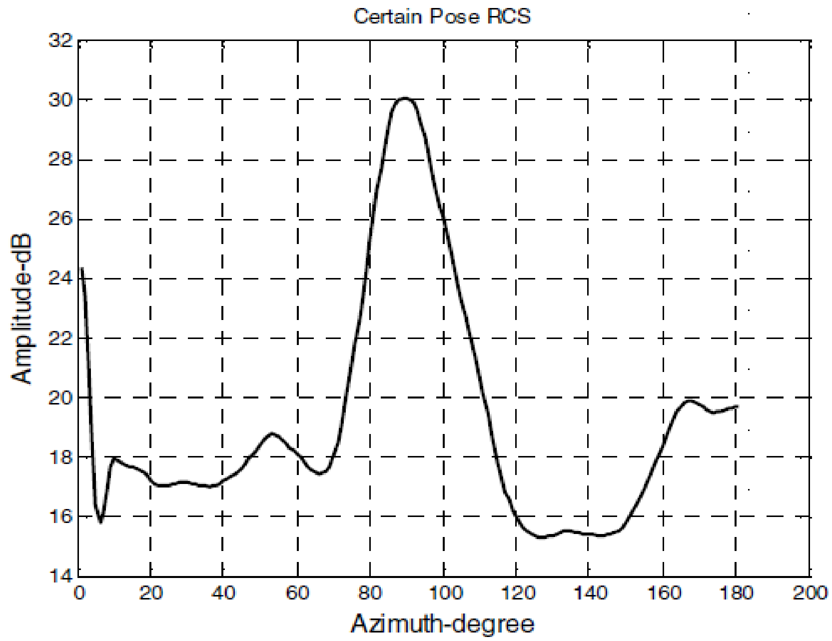

Figure 7 A target random pose Radar Cross Section *[23]*

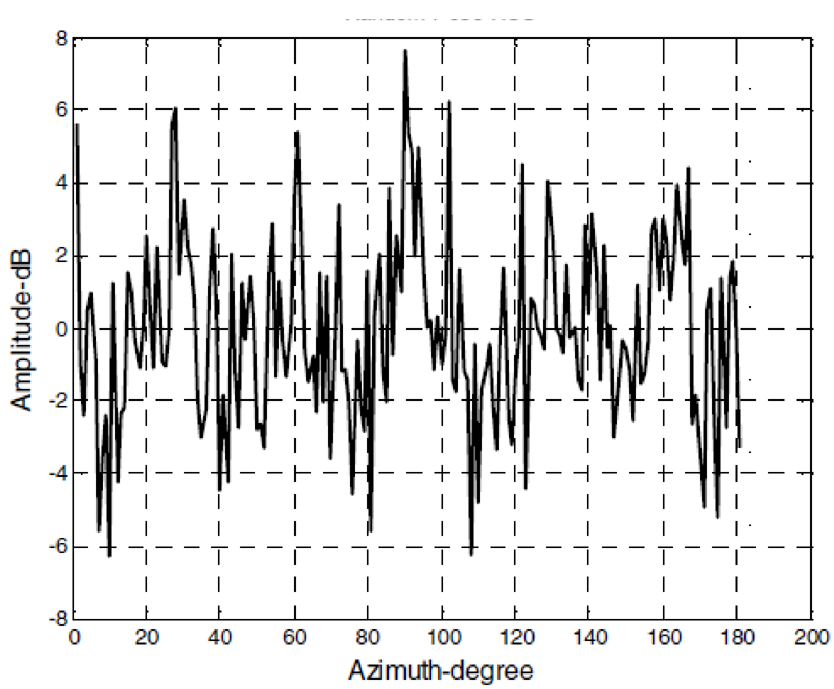

Figure 6 A target certain pose Radar Cross Section Curve *[23]*

The basic shape and frame of signal are indicated by the RCS sequence for a specific pose in these pictures. It expresses the signal's basic change current. The keystone of radar RCS signal processing is this.

"When the pitching is determined, the function between RCS and azimuth is shown in Figure 6. The function plot can be used to calculate the RCS in any pose. To improve target recognition, this can be utilized to create a target characteristic data warehouse. The function between the random posture RCS and the azimuth is shown in Figure 7. The noise characteristic is depicted in the graph.

The simulation demonstrates that wavelet filtering noise can be utilized to accurately decompose RCS signals. It also shows the breakup of the RCS sequence." [28]

3.1.5 RCS for Simple Objects

In theory, solving Maxwell's equations with proper boundary conditions will determine a target's RCS. However, this method can only be used to evaluate objects with basic geometries. The RCS of a simple conducting sphere as a function of the normalized circumference $2\pi a/\lambda$ where the radius is a, and the wavelength is denoted by λ. For this object the RCS can be divided into Rayleigh region "We define the Rayleigh region as that range in wavelength X or wave number k =2r/X for which the quantity of interest, be it scalar (acoustic) velocity potential, vector (electromagnetic) field, far zone field or scattering cross section, may be expanded in a convergent series in positive integral powers of k" [31] the Mie or the region of resonance and the optical region.

"In Rayleigh region, the RCS would vary by λ^4, where the size of the sphere is smaller compared with the wavelength. In the optical region, where the dimensions of the sphere are large compared with the wavelength, the RCS approaches a constant value πa^2. The RCS is oscillatory with frequency in the Mie or resonance region, which is located between the optical and Rayleigh regions. A target's RCS is determined by its aspect angle, frequency, and polarization. The physical environment plays a rather insignificant role in this context. The RCS of a conducting plate with a physical region is much greater than the wavelength when the object dimension is significantly greater than the wavelength. The product is given by:” [27] [26]

$$\sigma = G_e \cdot A = \frac{4\pi A}{\lambda^2} \cdot A = \frac{4\pi A^2}{\lambda^2} \tag{13}$$

3.1.6 Introduction to wavelet transform.

A Wavelet is a time-localized wave-like oscillation. Scale and place are the two most fundamental properties of wavelets. The scale (or dilation) of a wavelet determines how “stretched” or “squished” it is. This property has to do with how waves are described in terms of frequency. The wavelet's position in time is defined by its location (or space). Wavelet Transform is mapping from $L^2(R) \rightarrow L^2(R^2)$. The basic concept behind wavelet transforms is that they should only allow for changes in time extension, not shape. Choosing appropriate basis functions that allow for this has an impact on it. Changes in the time extension are supposed to correlate to the basis function's study frequency. Signal processing is based on the uncertainty principle. “The wavelet parameters (a, b) are then sampled on a grid or lattice to produce the discrete wavelet transform (DWT). The degree to which the signal can be reconstructed from its transform values is naturally determined by the sampling grid's coarseness. A fine grid mesh would allow for fast reconstruction, but at the cost of obvious redundancy, i.e., oversampling. A grid that is too coarse can result in data loss.” [29]

3.1.7 Continuous Wavelet Transform

Below we are presenting the Continuous wavelet transform defined in the equation in terms of dilations and by using Fourier Transform:

$$\psi_{ab}(t) = \frac{1}{\sqrt{a}}\psi\left(\frac{t-b}{a}\right) \leftrightarrow \Psi_{ab}(\Omega) = \sqrt{a}\Psi(a\Omega)e^{-jb\Omega} \tag{14}$$

This CWT maps a function given by *f(t)* into time scale space by:

$$W_f(a,b) = \int_{-\infty}^{\infty} \psi_{ab}(t) f(t) dt =< \psi_{ab}(t), f(t) > \qquad (15)$$

This transform is invertible if and only if the resolution of identity holds and is given by superstition (Klaunder and Sudarshan 1968)

$$f(t) = \underbrace{\frac{1}{C_\psi} \int_{-\infty}^{\infty} \int_{0}^{\infty} \frac{dadb}{a^2}}_{\text{summation}} \underbrace{W_f(a,b)}_{\substack{\text{Wavelet} \\ \text{coefficients}}} \underbrace{\psi_{ab}(t)}_{\text{Wavelet}} \qquad (16)$$

in which we have C_ψ equal to:

$$C_\psi = \int_{0}^{\infty} \frac{|\Psi(\Omega)|^2}{\Omega} d\Omega \qquad (17)$$

The wavelet is called asmissible if $C_\psi < \infty$ and this turn implies that the DC gain is $\psi(0)$ =0

$$\Psi(0) = \int_{-\infty}^{\infty} \psi(t) dt = 0 \qquad (18)$$

As a result, $\Psi(t)$ behaves like the impulse response of a band-pass filter with a decay rate at least equal to $|t|^{1-e}$. To provide strong time-localization, $\Psi(t)$ can decay much faster in practice.

3.1.8 Discrete Wavelet Transform

Redundancy and impracticality are two disadvantages of the continuous wavelet transform. “The first is obvious due to the wavelet transform's existence, while the second is due to the fact that both transform parameters are continuous. By sampling the parameters (a, b) and obtaining a set of wavelet functions in discretized parameters, we can attempt to solve both problems.” [29] A discrete wavelet transform (DWT) decomposes a signal into a number of sets, each set containing a time series of coefficients that describe the signal's time evolution in the corresponding frequency band. “Restricting the parameters *a* and *b* to represent discrete measures:

$a = m^{-j}$

$b = m^{-j} k$

where $j, k \epsilon Z, m \geq 2, m \epsilon Z^{+}$ and the DWT is defined as:

$$b(j,k) = m^{\frac{j}{2}} \int_{-\infty}^{\infty} f(t) \psi_{1,0}(m' - k) \mathrm{d}t \tag{19}$$

The mother wavelet is usually extended or compressed by powers of two when *m* is set to two. Higher multiplicity wavelets are described as wavelets with m ≥3. *m* will be set to two for the sake of illustration, with the generalization of larger values of m to follow. As a result, the mother wavelet's basis functions are now as follows:” [32]

$$\psi_{A,b}(t) = 2^{f} \psi_{1,0}(2j - k) \tag{20}$$

“The dilation and translation parameters are j and k, respectively. The mother wavelet can be obtained from a linear combination of scaling functions since the wavelet basis functions are constructed from dilations and translations of a mother wavelet. The mother wavelet is written as:” [33] [32]

$$\psi_{1,0}(t) = \sqrt{2} \sum_{k=-\infty}^{\infty} b_k \phi(2t - k) \tag{21}$$

- b_k high pass filter coefficents
- $\phi(t)$ scaling function that generates MRA multiresolution analysis with $\int_{-\infty}^{\infty} \phi(t)$ dt=1

If the scaling function generates a MRA than the scaling function satisfies the two scale difference equations where ℓ_k are low pass filter coefficients: $\phi(t) = \sqrt{2}\sum_{k=-\infty}^{\infty} \ell_k \phi(2t-k)$

The wavelet basis functions can be generated from the mother equation mentioned above and can be approximated with linear combination of basic functions of the wavelet, which is termed *wavelet decomposition off(t).*

$$f(t) = \sum_{j=-\infty}^{\infty} \sum_{k=-\infty}^{\infty} d_{j,k}\psi_{j,k}(t) \tag{22}$$

Extending the notation for the general m band, ($m \geq 2$) wavelet decomposition off*(t)* becomes:

$$f(t) = \sum_{s=1}^{m-1} \sum_{j=-\infty}^{\infty} \sum_{k=-\infty}^{\infty} d_{j,\boldsymbol{k}}^{(s)}\psi_{j,k}^{(s)}(t) \tag{23}$$

And mother wavelet equation also two scale different equation, become respectively:

$$\psi^{(s)}(t) = \sqrt{m} \sum_{k=-\infty}^{\infty} b_k^{(s)}\phi(mt-k), s = 1, \dots, (m-1) \tag{24}$$

$$\phi(t) = \sqrt{m} \sum_{k=-\infty}^{\infty} \ell_k \phi(mt-k) \tag{25}$$

The discrete version of the above equation is the DWT. Consider the DWT implementation algorithm. A filter can be thought of as the coefficients. A transformation matrix is used to apply the filter or coefficients to a raw data vector.

3.2. Application of wavelets to RCS

Simple objects as mentioned in the paragraph 3.2.1 are able to be approached by the decomposition technique. “Simple shapes are considered as the basis of the canonical forms which are used for the construction of the more complex targets such as a cylinder. The decomposition is performed on the target's polarization signatures as well as the phase and magnitude signatures. Each detail and approximation coefficients are linked in our method for any decomposition step. An inverse combination of these coefficients is used to recreate the original signal without sacrificing efficiency. The approach is based on an empirical selection of relevance zones of the RCS” [9]

3.2.1 Quantitative Selection of an RCS's Relevance Zones

Two stages of decomposition are used in our process. “The mother wavelet is a symmetric wavelet, as the RCS of a simple target has symmetric properties. Any simple shape's RCS is determined by the relative size of each of its geometrical features in relation to the incident field wavelength. An empirical way to characterize the influence of these features consists in varying one target’s dimension while others are frozen to an arbitrary value.” [9]

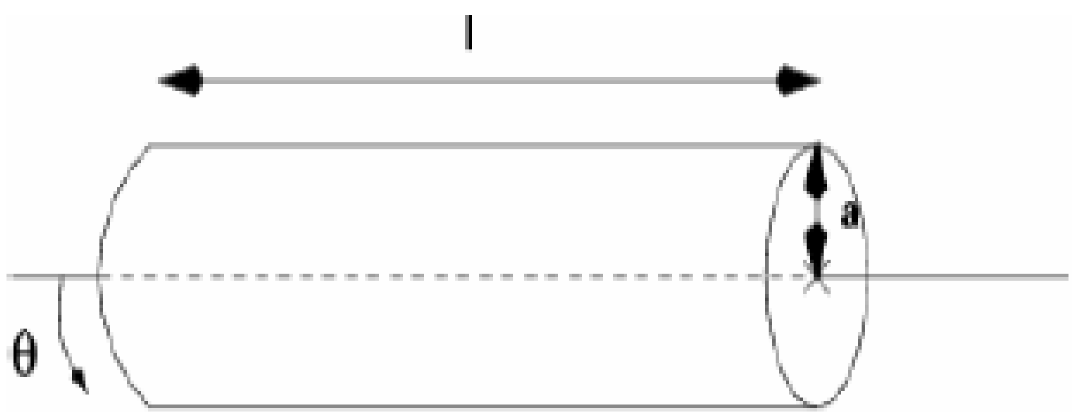

Figure 8 Geometry of a right circular cylinder used to compute RCS. *[9]*

“To locate the null points of the first derivate of the signal, the discrete wavelets transform (DWT) is first applied to the RCS. The number of these points is high if the number of variations in the signal is significant, and they correspond to the transition points between the different phases of the signal. The contribution of each simple entity that could be considered a constituting part of the more complex target is taken care of using the discrete wavelet decomposition on the final RCS for complex targets.” [34]

There are two options to consider:

1. If the characterization ranges of each of the complex target's simple forms do not overlap, the procedure mentioned above can be used to evaluate the size of each simple object.

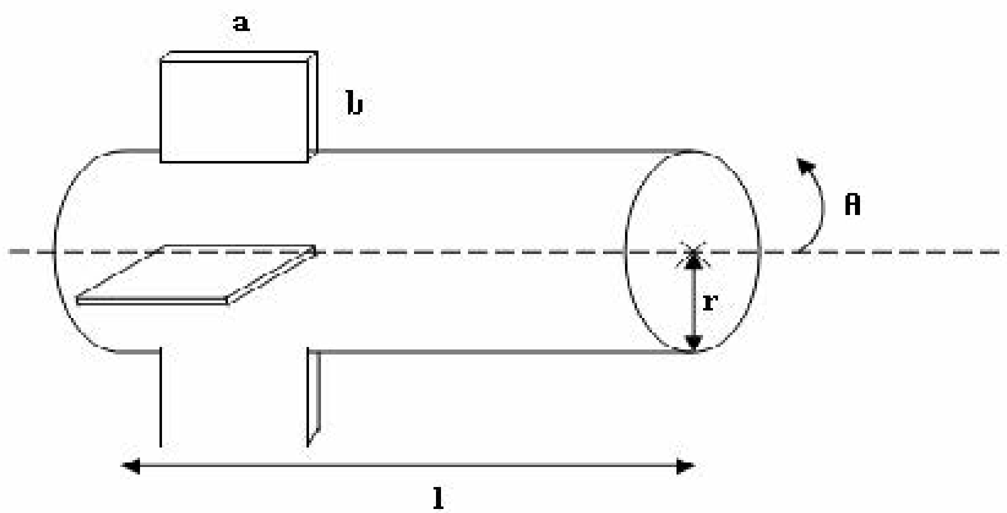

Figure 9 Complex target example, Cylinder with Fins *[9]*

2. If any characterization sets of canonical forms overlap, this indicates that "data fusion" has occurred.

Two discrete wavelet transforms are applied in succession to identify the entity whose contribution to the entire RCS is the most significant. As a result, the detail coefficients of the second level describe the canonical form that contributes the most to the signal.

3.2.2 Application on simple Targets

To find the unique parameters that characterize each target, wavelet decomposition is applied to each RCS signal of a cylinder of length L and radius a. After the RCS has been computed using the geometrical principle of diffraction, this decomposition method is used (GTD).
As shown in Figure 10, the monostatic pattern of a right circular cylinder has symmetric characteristics. “This pattern has four specular lobes: one in the middle, one split on both sides of the 2π map, which corresponds to the flat circular ends of the cylinder, and the

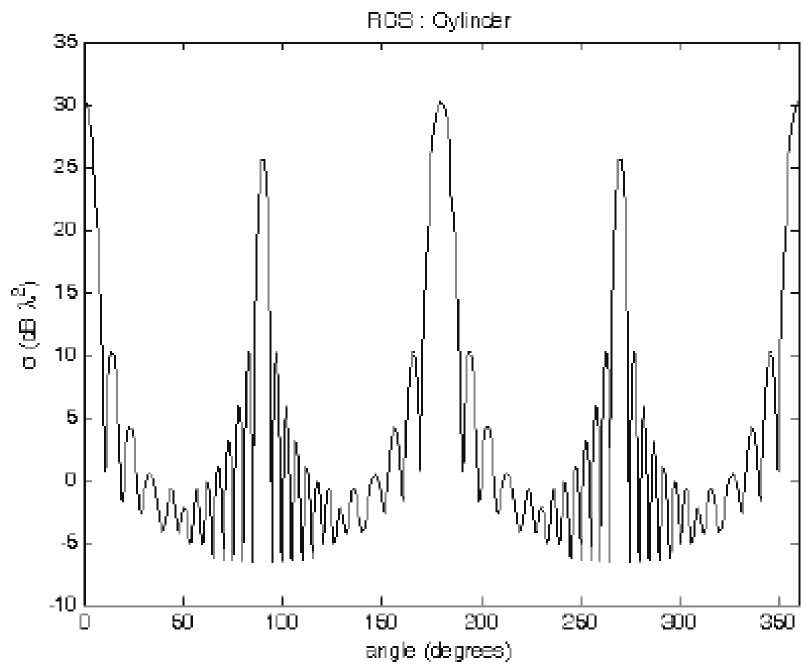

Figure 10 RCS pattern of a right circular cylinder at frequency 0.3GHz for vertical indicent polarization between 0 and 2π *[9]*

ones at $\pm\pi/2$, which correspond to the specular echoes from its curved sides.” [9]

Thus, the two lobes at angles of $\phi=0$ and $\phi=\pi$ correspond to the cylinder's circular ends (the cylinder appears as a disk at these angles) and thus define its radius.

Similarly, lobes at an angle of $\phi=\pm\pi/2$ provide an estimate of the cylinder's length (ie., the influence of the radius dimension due to the curved sides of the cylinder is negligible).

3.2.3 Application on Complex Targets

A complex target is believed to have a finite number of significant scattering centers wherever possible, resulting in an appropriate signature of N components for the complex target. Each contribution of a simple object can be evaluated using discrete wavelet decomposition on the final RCS. However, determining the scattering centers of complex targets analytically is a difficult task. As an example, the cylinder with four blades shown in Figure 10 “can be considered a sum of canonical shapes, and a certain number of dominant scattering centers can be identified depending on the directions of incidence and observation of the high frequency signal. By adding the contributions from all of the scattering centers that could be allocated to each simple form, the entire RCS of this objective is approximated.” [9]

3.2.4 Image processing with wavelet transform.

Wavelet’s methods employ a flexible window to interpret data at multiple sizes or resolutions, which makes them fascinating and useful for singularity identification and signal characterization. In the time-scale domain, the results of the continuous wavelet transform are frequently represented graphically and shown as two-dimensional images. The pictures of the L^2-function under the continuous wavelet transform produce a reproducing kernel Hilber space that can be used in a variety of applications.

The scattering mechanisms that characterize the behavior of objects in radar systems to incident waves can be divided into two types: dispersive and non-dispersive scattering mechanisms. Local scattering features can be retrieved from the local maxima of the target response in the time domain for non-dispersive scattering such as corners, edges, or specular reflections.

Based on the geometrical theory of diffraction, the backscattered field recorded by a linearly polarized receiving antenna of the radar system can be expressed as follows:

$$\vec{E}(\mathrm{k}, z) = \sum_{n=1}^{N} \mathrm{A_n}(\mathrm{jk})^{\gamma\mathrm{n}} \exp\left(-\mathrm{j2k}\hat{z} \cdot \vec{r}_{\mathrm{n}}\right) \tag{26}$$

Where:

$\mathrm{A_n}$ is weighting coefficient; $\gamma\mathrm{n}$ is a real number which corresponds to the geometry of n-th scattering center; $(\mathrm{jk})^{\gamma\mathrm{n}}$ are components dependent on frequency that describe diffractation and reflection; $\hat{z} \cdot \vec{r}_{\mathrm{n}}$ denotes with respect to a phase reference the range of n-th scatter; c is the speed of light; $\hat{z}$ is the unit vector in Z direction.

“The backscattered data corresponding to the wave number sample k is given by, after normalizing the field to a particular polarization and normalizing the term $(\mathrm{jk})^{\gamma_{\mathrm{n}}}$ to a central reference wave number k_r in order to achieve the same unit for $(\mathrm{jk})^{\gamma_{\mathrm{n}}}$ for any value of yn” [26]:

$$\begin{aligned} \mathrm{E(k)} &= \sum_{n=1}^{N} \mathrm{A_n}(\mathrm{jk}/\mathrm{k_r})^{\gamma_{\mathrm{n}}} \exp\left(-\mathrm{j2k}\hat{z} \cdot \vec{r}_{\mathrm{n}}\right) \\ \mathrm{E(k)} &= \sum_{n=1}^{N} \mathrm{A_n}(\mathrm{jk}/\mathrm{k_r})^{\gamma_n} \exp\left(-\mathrm{j2k}\zeta_{\mathrm{n}}\right) \end{aligned} \tag{27}$$

Where ζ_{n} is the projection of $\vec{r}_{\mathrm{n}}$ in the z direction? The signal E(k) is represented by the wave number k with the dimension radian/length (rad/m), and the range domain solution is found by transforming it to the range domain with the dimension length (meter).

When we transform Continuous, Wavelet Transform in the k domain, and shift it accordingly in a central wave number (center the signal) we get the following equation:

$$\begin{aligned} \mathrm{CWT}\ (a,b) &= [(\sqrt{a})/(2\pi)]\int_{-\infty}^{+\infty}\sum_{n=1}^{N}|A_n|\exp\,(j\phi_n) \\ &k_r-\gamma_n k^{\gamma_n}\exp\,\{j[\pi\gamma_n/2-2k\zeta_n]\}\Phi(ak)\exp\,(jbk)dk \\ &= [(\sqrt{a})/(2\pi)]\exp\,\{j[\pi\gamma_n/2]\}\sum_{n=1}^{N}|A_n|\exp\,(j\phi_n) \\ &k_r^{-\gamma_n}\int_{-\infty}^{+\infty}k^{\gamma_n}\Phi(ak)\exp\,\{jk[b-2\zeta_n]\}dk \end{aligned} \tag{28}$$

and by centering it we get:

$$\begin{aligned} \mathrm{CWT}(\mathrm{a},\zeta) &= [(\sqrt{a})/(2\pi)]\exp\,\{\mathrm{j}[\pi\gamma_\mathrm{n}/2]\}\sum_{n=1}^{N}|\,\mathrm{A_n}|\exp\,(\mathrm{j}\phi_\mathrm{n}) \\ &\mathrm{k_r^{-\gamma_n}}\int_{-\infty}^{+\infty}\mathrm{k}^{\gamma\mathrm{n}}\Phi(\mathrm{ak})\exp\,\{\mathrm{jk}[\zeta-\zeta_n]\}\mathrm{dk} \end{aligned} \tag{29}$$

The last equation is Inverse Fourier Transform of the function $\{k^{\gamma_n}\Phi(ak)\}$ with scale range domain *c/2δf* where *δf* is frequency step of the radar system. The result that we would get is a 2-D image. To process this approach, the image would be sliced along scale axis into many pieces to obtain a multi resolution range profile.

The local modulus maxima algorithm can then extract local features from the significant range profile (a slice of the scale-range image corresponding to a specific scale proportional to the number of frequency samples in the observation). These features are crucial information about scattering centers, which can be used for automatic target recognition.

3.3 Radar Response Analysis to Time-Frequency Method

“The scattering analysis of radar targets is done using four different time-frequency analysis approaches. In scattering analysis, the Short-Time Fourier Transform (STFT), Continuous Wavelet Transform (CWT), Adaptive Wavelet Transform (AWT), and

Evolutionary AWT (EAWT) are used. Scattering centers and resonance frequencies are two scattering phenomena that are crucial for radar target signature analysis. The comparisons of four alternative time-frequency analysis techniques are provided in the simulation using wire target data. We can acquire target scattering properties such as scattering centers and natural resonance frequencies by analyzing the radar scattered response." [12]

"The radar signal is made up of two parts: an early-time response and a late-time response. The early-time response contains information about the scattering centers, which are aspect dependent, whereas the late-time response contains information about the natural resonance frequencies, which are aspect independent and solely dependent on target geometry. The time-domain analysis and the frequency-domain analysis can both be used to analyze radar signals. We can extract the scattering center information using time domain analysis, such as a range profile. The spectrum of a radar signal, on the other hand, can represent the target resonance frequencies. Recently, time-frequency (T-F) analysis methods are developed. T-F analysis can represent these two features simultaneously." [12]

To examine the non-stationary radar signal, various T-F transformations were created. The short-time Fourier transform (STFT), Wigner-Ville distribution (WVD), continuous wavelet transforms (CWT), and adaptive wavelet transform are all well-known approaches (AWT).

"The STFT is the most common and fundamental T-F analysis. The STFT is simple and straightforward to use, although it has a resolution issue. Although the WVD has a higher resolution than the STFT, it suffers from a cross-term (ghost) problem. Although the CWT includes a multi-resolution feature, its time-frequency grid remains rigid. Compared to the CWT, the AWT has a more flexible time-frequency grid. The STFT, WVD, and CWT are non-parametric analysis tools, whereas the T-F analysis is parametric. It is also unaffected by the resolution and cross-term problems. The fast Fourier transform (FFT) and bisection search method are used in the traditional AWT." [12]

3.3.1 Short Time Fourier Transform

The primary method for studying nonstationary signals is the STFT. The signal is separated into small segments in STFT, with these segments being believed to be stationary. A window function is employed for this reason. In time domain Small Time FT is:

$$STFT(\tau,\Omega) = \int_{-\infty}^{\infty} [f(t)w^*(t-\tau)]\exp(-j\Omega t)dt \tag{30}$$

w(t) is a window function and f(t) are a time-domain signal. The uncertainty principle, which is a window trade-off condition, affects the STFT. Long time windows offer good frequency resolution but not so much temporal resolution. Time resolution is acceptable with short time windows, but frequency resolution is weak.

3.3.2 Continuous Wavelet Transform

"The CWT was created as an alternative to the STFT in order to solve the resolution difficulty. The specular return in the early-time stage and the resonances at the late-time stage make up the scattered response of a target in general. It is preferable to employ good time resolution in the early time and good frequency resolution in the late time to extract this information simultaneously." [12]

$$CWT_f(\tau,\Omega) = \sqrt{\tau}\int F(\omega)\Psi\big(\tau(\omega-\Omega)\big)d\omega \tag{31}$$

In order to create a CWT, many different wavelet functions might be employed as prototypes. Because the Morlet wavelet is so useful for extracting scattering processes, we employ it as the mother wavelet.

3.3.3 AWT and EAWT

"Instead of FFT and the bisection method used in conventional AWT, evolutionary AWT (EAWT) uses evolutionary programming (EP) for T-F parameter extraction. As a result, we refer to this algorithm as Evolutionary AWT. First, we will go through the conventional AWT. The time domain measured data s(t) is extended as follows using the usual AWT.” [12]

$$s(t) = \sum_{m=1}^{\infty} B_m h_m(t) \tag{32}$$

Where:

$$h_{\mathrm{w}}(t) = (\pi\sigma_{\mathrm{m}}^2)^{-02s} \mathrm{exp}\left\{-\frac{(t-t_{\mathrm{si}})^2}{2\sigma_{\mathrm{m}}^2}\right\} \mathrm{exp}\,(j2\pi f_{\mathrm{m}} t) \tag{33}$$

“In AWT algorithm σ_{m} is an adjustable standard deviation; time frequency center t_m, F_M and amplitude B_m are obtained such that $h_m(t)$ is most similar to $S_{m-1}(t)$:” [12]

$$|B_m|^2 = \max_{t_m, f_m, \sigma_m} \left|\int s_{m-1}(t) h_m^*(t) dt\right|^2 \tag{34}$$

“Where $s_0(t)$= s(t). For m > 1, $s_{m-1}(t)$I s the remainder after the orthogonal projection of $s_{m-1}(t)$ onto $h_m(t)$ has been subtracted from the signal. Solution of the above signal is found using FFT and bisection search method. While EAWT extracts these parameters using evolutionary optimization.” [12]

CHAPTER 4
METHODOLOGY

This research has been based on a MATLAB example which is also referred on the reference section [3]. This example demonstrates how to identify radar returns using machine learning and deep learning techniques. Wavelet scattering feature extraction and a support vector machine are used in the machine learning methodology. Two deep learning algorithms are demonstrated: transfer learning using SqueezeNet and a recurrent neural network with Long Short-Term Memory (LSTM). Although the data set in this case does not necessitate advanced techniques, the workflow is given because the approaches can be applied to more difficult challenges.

We choose to base our methodology in this experiment but changing the transfer learning net, using RESNET50 instead. We also compared the training time and differences between SqueezeNet and ResNet. The steps to our experiment are explained in detail in the sections below.

4.1 Radar Cross Section Synthesis

This section explains how to generate synthesis data for use in training learning algorithms. The RCS pattern of a cylinder with a radius of 1 meter and a height of 10 meters is simulated. The radar's operating frequency is 850 MHz. From the input of this data, we create a synthesized data train, as presented in images 11 and 12.

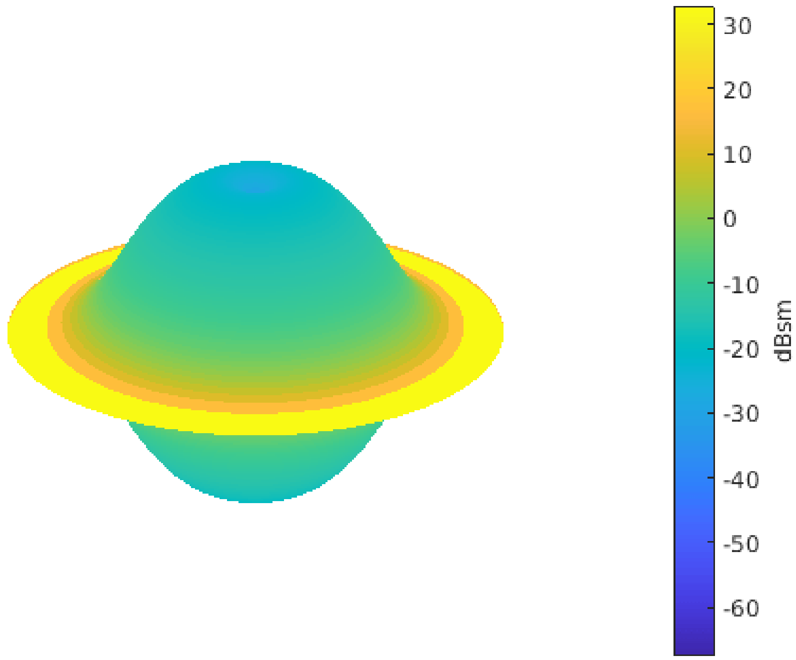

Figure 11 Data Train

From the pattern that we create, we than apply a backscatter radar target to reproduce returns from various aspects angles by using `phased. BackscatterRadarTarget` which models the backscattering of a signal from a target. When the incident and reflected angles are the same, backscattering is a specific case of radar target scattering. Monostatic radar designs are affected by this form of dispersion. The backscattering response of a target to an incoming signal is determined by the radar cross-section. This System object allows the definition of a radar cross-section model that is angle-dependent and covers a wide range of incident angles. When we run the function of phased. BackscatterRadarTarget, we get the Propagation speed of the target, the operation frequency, Azimuth angles, Elevation angles and RCS pattern.

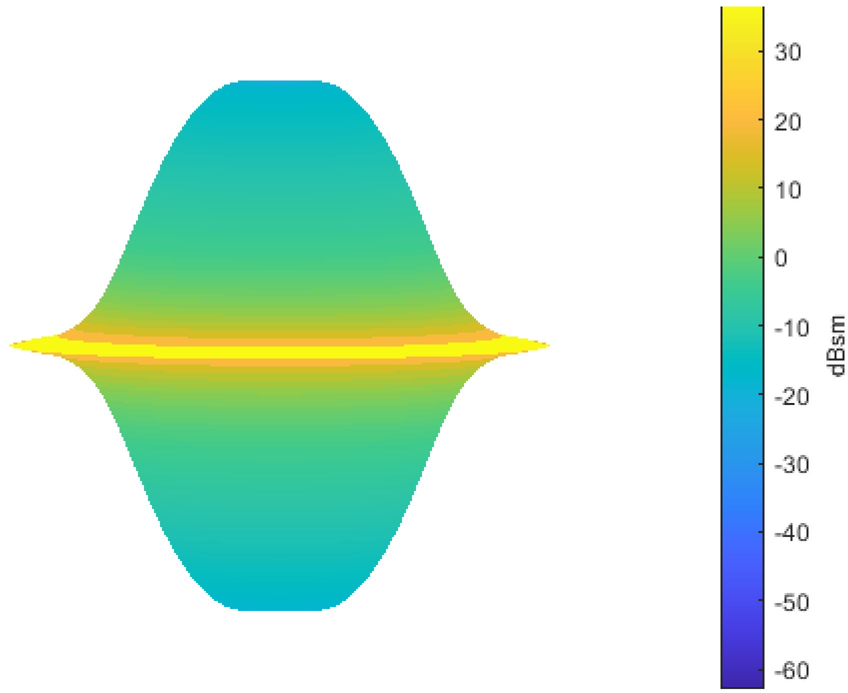

Figure 12 Different angle of figure 11

If we simulate 100 returns of the cylinder, as a result of the cylinder's motion, minor vibrations surrounding the bore sight cause the aspect angle to shift from one sample to the next as shown in figure 13 and 14. The plot in this picture has N equal to 100, for cylinder returns, azimuth angle and elevation angle are randomly generated, and the plot has time Index and Target return in Decibel.

The cone's return can be formed in the same way. To create a training set, the process explained above for target return and cone return is repeated 5 different times for different cylinder radii. In addition, 10 motion profiles are simulated for each radius by altering the incident angle while tracking 10 randomly generated sinusoids around the boresight. Each motion profile contains 701 samples, resulting in 701-by-50 samples. The procedure is repeated for the cylinder target, yielding a 701-by-100 training data matrix including 50 cylinder and 50 cone profiles. To generate a 701-by-50 training set in the test set, we used

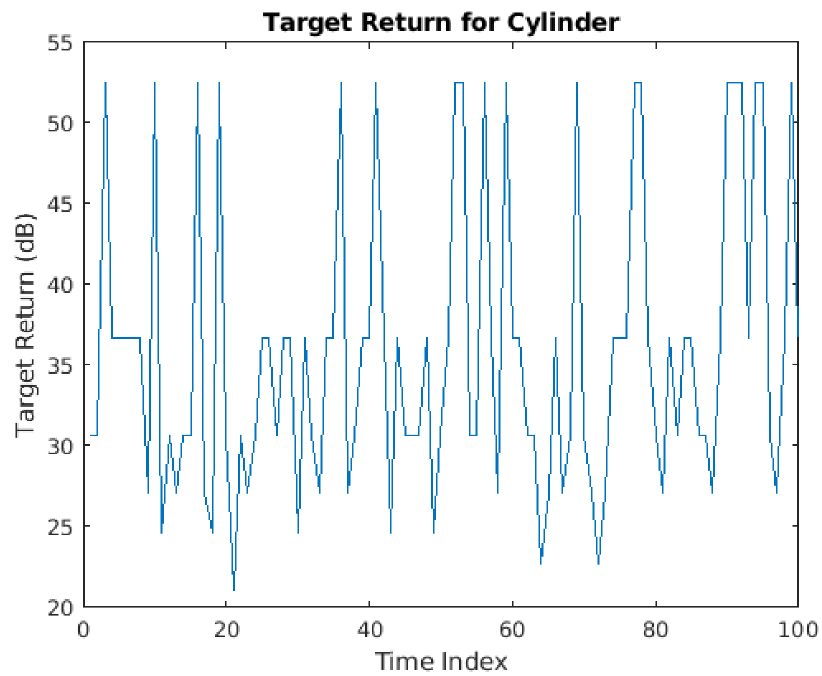

Figure 14 Target Return for N=100

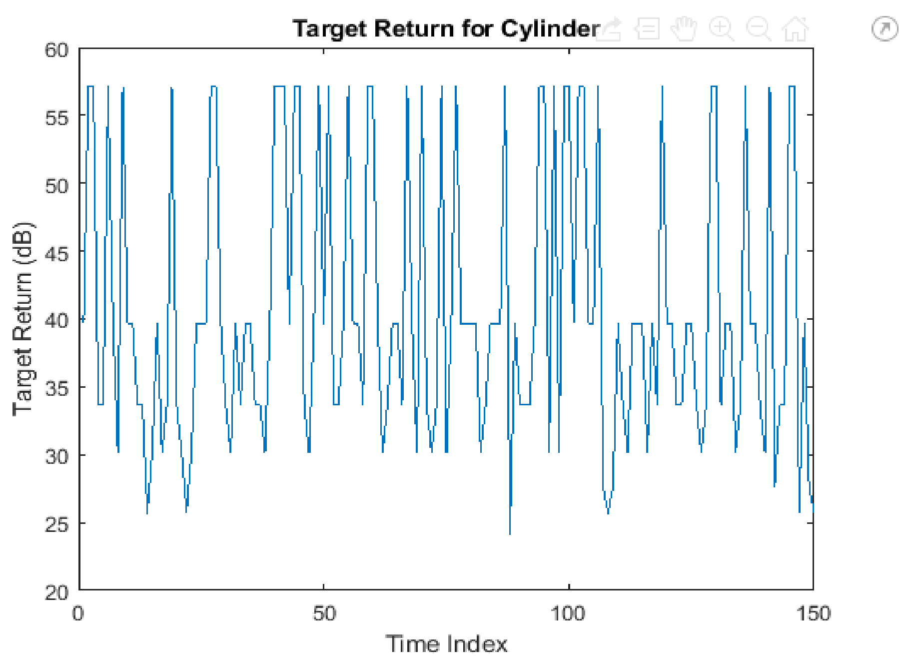

Figure 13 Target Return for cylinder, example with N=150

25 cylinder and 25 cone profiles. The training data is precomputed and loaded below due to the long computation time. By doing this we create training data for RCS Return.

The next graphic figure 15, displays the return for one of each shape's motion profiles. Both the incidence azimuth angles, and the target returns are plotted to show how their values fluctuate over time. In this plot the limits of y-axis are set to -50 to 50 and represent Azimuth and Aspect angle for cylinder and cone, and their target Return in dB.

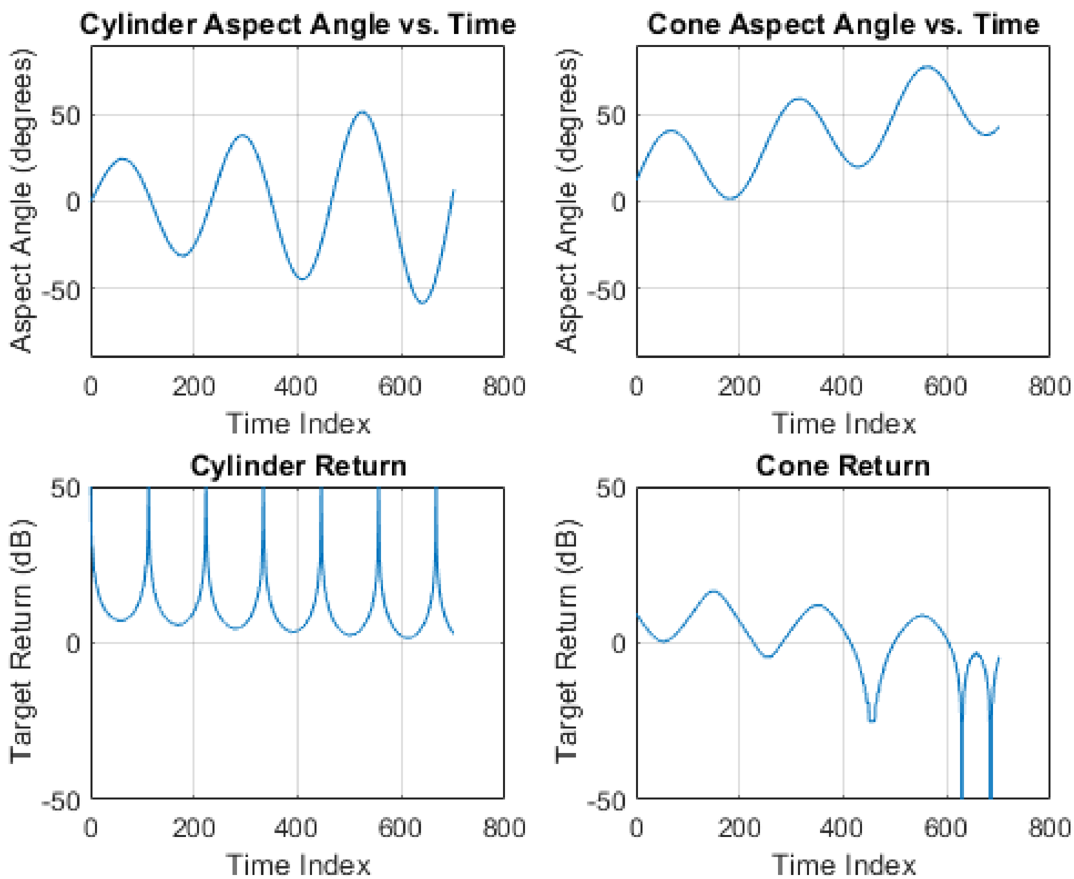

Figure 15 Return of the motion profile for each shape

4.2 Wavelet Scattering

Data is transmitted through a succession of wavelet transforms, nonlinearities, and averaging in the wavelet scattering feature extractor to obtain low-variance representations of time series. Wavelet time scattering produces signal representations that are insensitive to input signal shifts while maintaining class discriminability. We created a network for a wavelet time scattering decomposition using the Gabor (analytic Morlet) wavelet with the waveletScattering object. To construct low-variance representations of real-valued time series data, the network employs wavelets and a lowpass scaling function. Next, we obtain the training transform from the training set and test set. Then we create labels for training and for learning divided in: Cylinder and Cone 50 labels per each in the training set, and 25 labels per each in the test set.

4.3 Model Training

To get the cross-validation accuracy, we fit a support vector machine model (SVM) with a quadratic kernel to the scattering features. We fit multiclass models for support vector machines or the training set. And we use it to validate the accuracy of the training labels and the training features that we got from the wavelet scattering. The output is 100% validation accuracy. This gives us clearance to continue with the target classification.

4.4 Target Classification

We used the trained Support Vector Mechanism mentioned before to classify the scattering featured from the test set. We predict Labels and plot the accuracy. The accuracy is 100%.

Then we plot a confusion matrix which uses the test labels and training data. The figure below (figure 16) displays the output. From our prediction, as we can see in the figure below, the accuracy of predicted Cone or Cylinder would be 100% and the predicted labels accuracy would also be 100%.

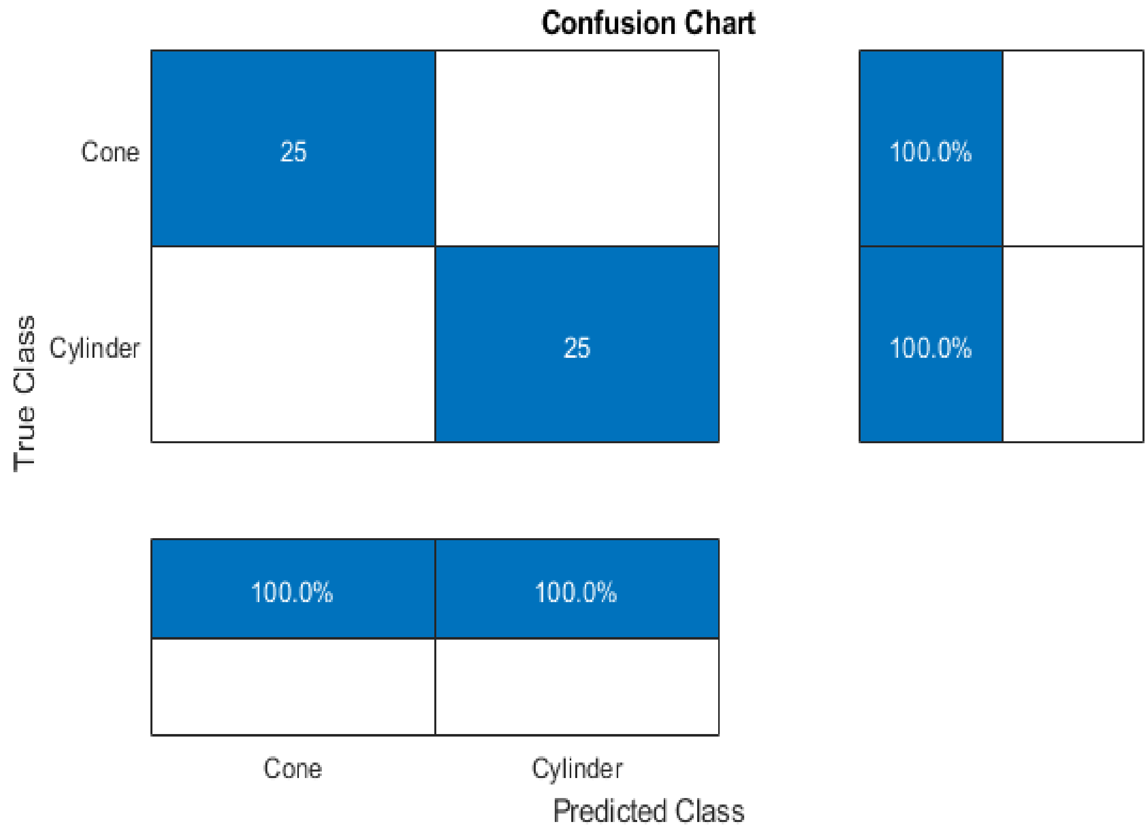

Figure 16 Prediction Chart

4.5 Transfer Learning with Resnet50

ResNet-50 is a 50-layer deep convolutional neural network. a pre-trained version of the network can be loaded from the ImageNet database, which has been trained on over a million photos. This network can classify images into 1000 object categories, and it consists of 177 layers. The network's picture input size is 224 × 224 × 3. SqueezeNet on the other hand, has 68 layers. Like all DCNNs, it uses a cascade of convolutional operators, nonlinearities, and pooling, or averaging. SqueezeNet anticipates a 227-by-227-by-3 picture input. We load ResNet as shown in image 17 and we get layers supplemented with their features as is also shown in image 18.

```
resnet50
```

```
ans = 

  DAGNetwork with properties:

         Layers: [177×1 nnet.cnn.layer.Layer]
    Connections: [192×2 table]
```

Visualize the network using Deep Network Designer.

Figure 17 Load Resnet50

```
snet =resnet50
```

```
snet = 
  DAGNetwork with properties:

         Layers: [177×1 nnet.cnn.layer.Layer]
    Connections: [192×2 table]
     InputNames: {'input_1'}
    OutputNames: {'ClassificationLayer_fc1000'}
```

```
snet.Layers
```

```
   159   'activation_45_relu'           ReLU                      ReLU
   160   'res5b_branch2c'               Convolution               2048 1×1×512 convolutions with stride [1  1] and padding [0  0  0  0]
   161   'bn5b_branch2c'                Batch Normalization       Batch normalization with 2048 channels
   162   'add_15'                       Addition                  Element-wise addition of 2 inputs
   163   'activation_46_relu'           ReLU                      ReLU
   164   'res5c_branch2a'               Convolution               512 1×1×2048 convolutions with stride [1  1] and padding [0  0  0  0]
   165   'bn5c_branch2a'                Batch Normalization       Batch normalization with 512 channels
   166   'activation_47_relu'           ReLU                      ReLU
   167   'res5c_branch2b'               Convolution               512 3×3×512 convolutions with stride [1  1] and padding 'same'
   168   'bn5c_branch2b'                Batch Normalization       Batch normalization with 512 channels
   169   'activation_48_relu'           ReLU                      ReLU
   170   'res5c_branch2c'               Convolution               2048 1×1×512 convolutions with stride [1  1] and padding [0  0  0  0]
   171   'bn5c_branch2c'                Batch Normalization       Batch normalization with 2048 channels
   172   'add_16'                       Addition                  Element-wise addition of 2 inputs
   173   'activation_49_relu'           ReLU                      ReLU
   174   'avg_pool'                     Global Average Pooling    Global average pooling
   175   'fc1000'                       Fully Connected           1000 fully connected layer
   176   'fc1000_softmax'               Softmax                   softmax
   177   'ClassificationLayer_fc1000'   Classification Output     crossentropyex with 'tench' and 999 other classes
```

Figure 18 Resnet50 Layers

4.6 Convolutional Neural Network & Transfer Learning

ResNet50 is a neural network that can detect and identify changes in photos. As a result, we must convert the 1-D radar return time series into an image in order to apply this transfer learning net to classify radar returns. There are several options for a signal's time-frequency representation, and which one is best depends on the signal's properties. To figure out which TFR is best for this scenario, a few radars return from were picked from each class randomly and then plotted.

After we transformed the radar returns in images, the radar returns previously displayed are clearly characterized by gradually varied changes interrupted by huge transitory drops, as previously stated. To sparsely represent such signals, a wavelet transform is optimal. Wavelets decrease to capture slowly evolving signal structure and stretch to locate transitory occurrences with high temporal precision. Fig 19 and 20.

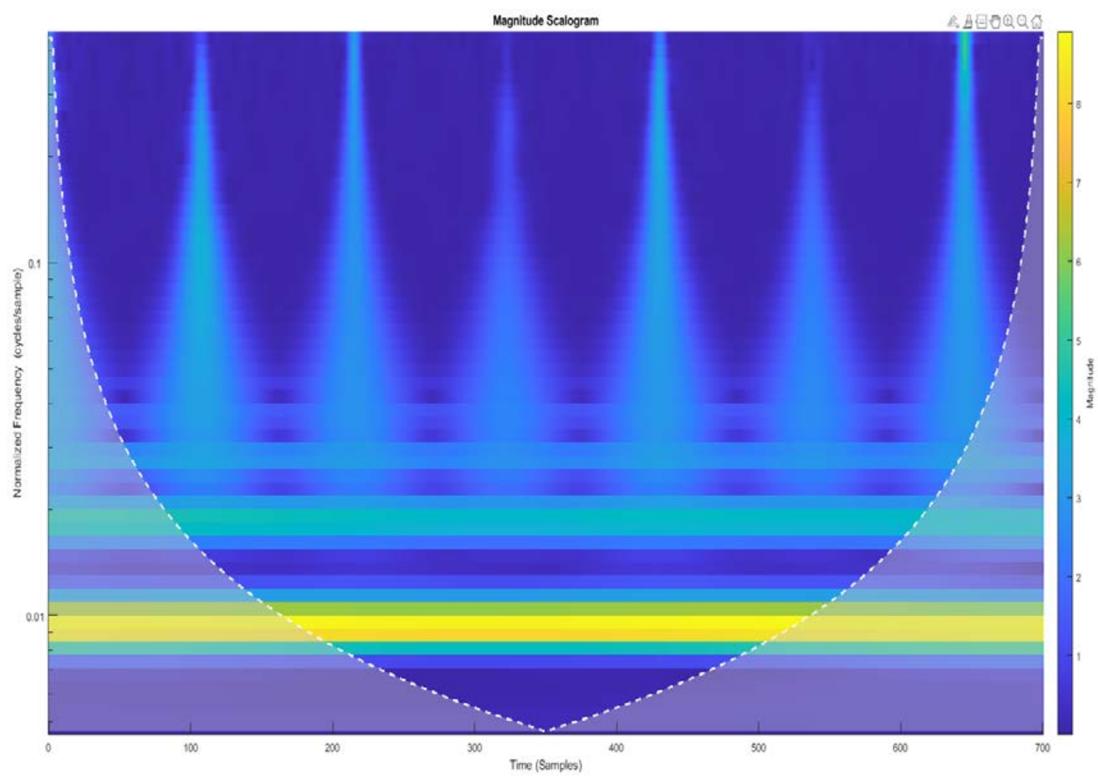

Figure 19 Magnitude Scalogram for Cylinder Returns

We choose the CWT as the optimum TFR to utilize since the transients appear to be crucial in distinguishing whether the target return is from a cylinder or cone target.

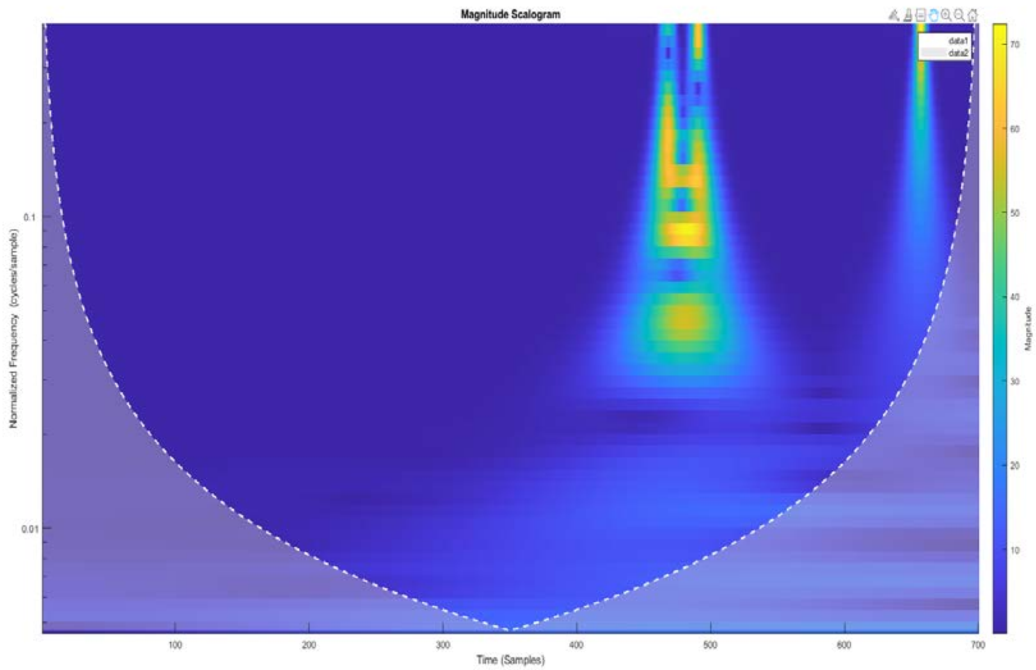

Figure 20 Magnitude Scalogram for Cone Returns

We create images from each radar return's CWT after getting the CWT for each target return. We scale these photographs to make them suitable with the Resnet input layer, and then use Resnet to classify the results.

4.7 Image Preparation

We use helpergenWaveletTFImg to make the image preparation, by also using Image Processing Toolbox. We change the layer 175 of Resnet to have the same number of 1x1 convolutions, then we retrain Resnet50. To train this network we can use trainNetwork which will automatically use the GPU. TrainNetwork uses the CPU if there is no compatible GPU available and training should take about five minutes. Training times differ depending on a variety of circumstances. The training takes place on a CPU in this scenario because the ExecutionEnvironment parameter is set on CPU. Figure 21 displays RCS returns Classification predictions.

We than retrain Resnet and set the initial learn rate to 1e-4 and the max number of epochs is set to 15 while minibatch is 10.

```
ans =

  ClassificationOutputLayer with properties:

            Name: 'ClassificationLayer_predictions'
         Classes: [1000×1 categorical]
      OutputSize: 1000

   Hyperparameters
    LossFunction: 'crossentropyex'

Generating Time-Frequency Representations...Please Wait
   Creating Cylinder Time-Frequency Representations ... Done
   Creating Cone Time-Frequency Representations ... Done
   Creating Cylinder Time-Frequency Representations ... Done
   Creating Cone Time-Frequency Representations ... Done
```

Figure 21 Layers Classification

Epoch	Iteration	Time Elapsed (hh:mm:ss)	Mini-batch Accuracy	Mini-batch Loss	Base Learning Rate
1	1	00:00:17	60.00%	0.8539	1.0000e-04
5	50	00:06:34	100.00%	0.0250	1.0000e-04
10	100	00:11:38	100.00%	0.0120	1.0000e-04
15	150	00:18:10	100.00%	0.0087	1.0000e-04

Figure 22 Epoch Iterations Resnet50

The values and time for each iteration changes between Resnet and SqueezeNet. In Resnet, one iteration needs more time to be run. In image 23 it can be seen the Iteration process for SqueezeNet.

```
Initializing input data normalization.
|========================================================================================|
|  Epoch  |  Iteration  |  Time Elapsed  |  Mini-batch  |  Mini-batch  |  Base Learning  |
|         |             |   (hh:mm:ss)   |   Accuracy   |     Loss     |      Rate       |
|========================================================================================|
|       1 |           1 |       00:00:02 |       60.00% |       2.6639 |      1.0000e-04 |
|       5 |          50 |       00:01:10 |      100.00% |       0.0001 |      1.0000e-04 |
|      10 |         100 |       00:02:20 |      100.00% |       0.0002 |      1.0000e-04 |
|      15 |         150 |       00:03:41 |      100.00% |   2.2240e-05 |      1.0000e-04 |
|========================================================================================|

accuracy =

   100
```

Figure 23 SqueezeNet Iteration process

Also, if we compare the processes for Resnet50 and for SqueezeNet we see a big difference in time. The images below, Have a clear difference in the training process also.

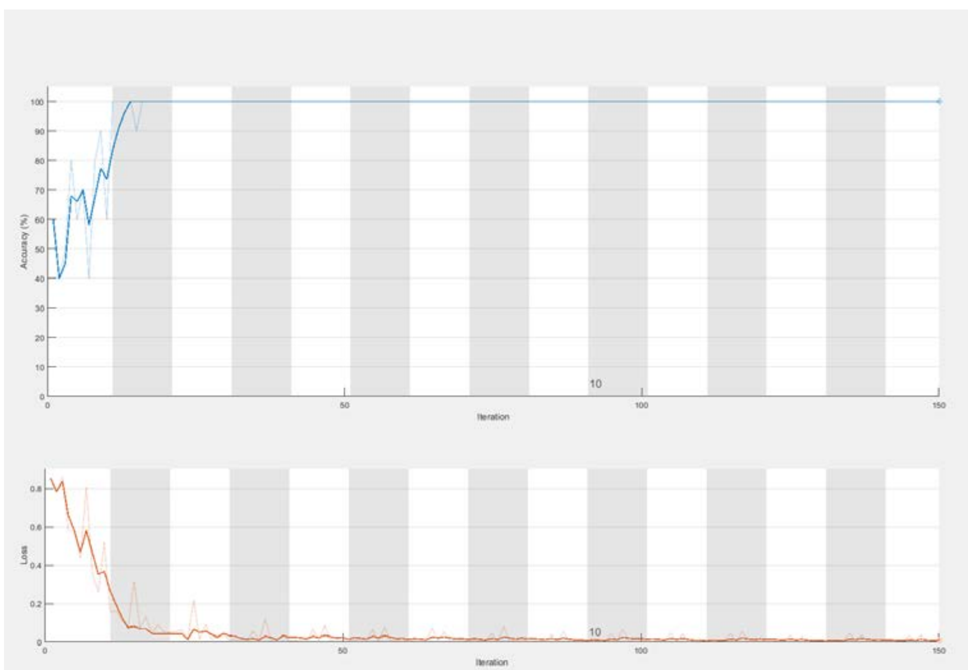

Figure 24 Resnet Training process

From the images 24 and 25 we recognize that the training curve in the first iterations for resnet50 is alternated. Furthermore, the images below (26 and 27) illustrate are presented results and time for both processes. Resnet is slower but both of them complete the process successfully.

After the training and test samples are run, we plot again the confusion chart of prediction, and the results are the same with image 16. The prediction is 100% accurate.

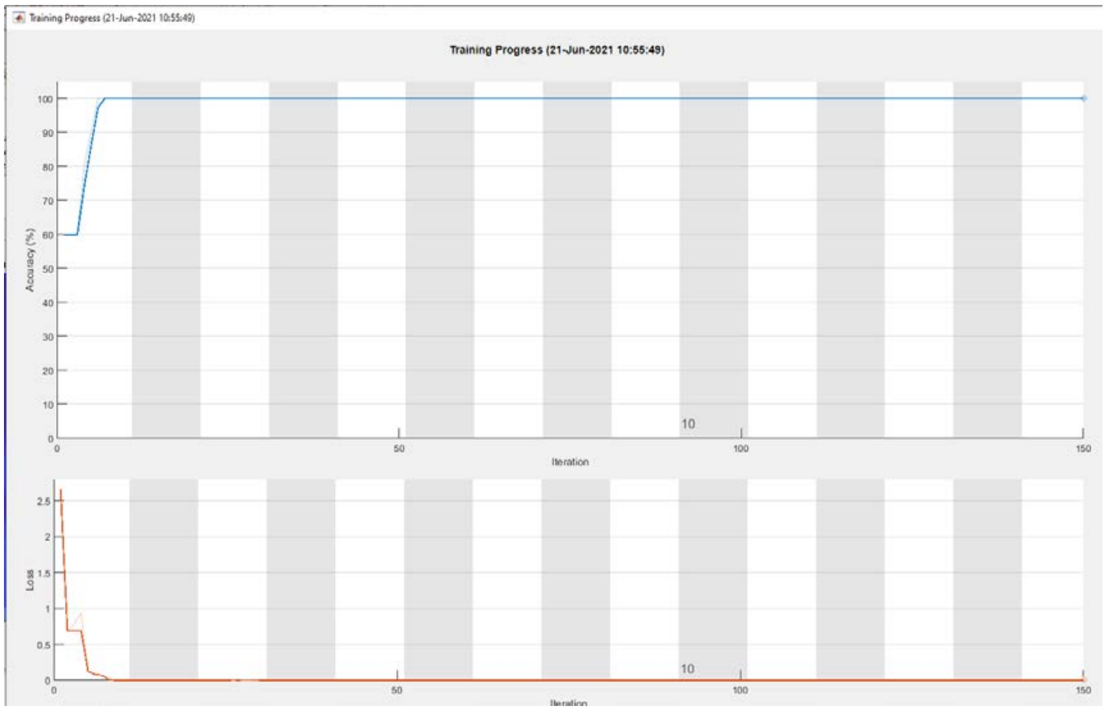

Figure 25 SqueezeNet Training process

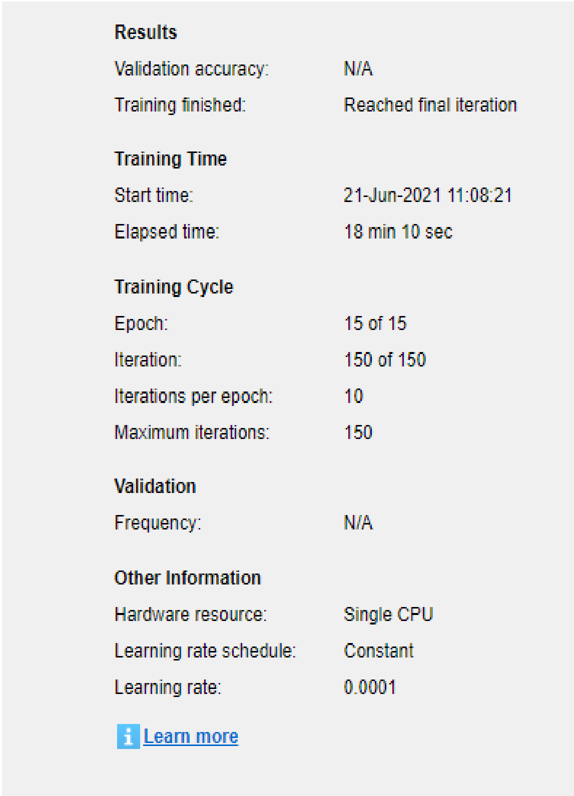

Figure 26 Resnet results

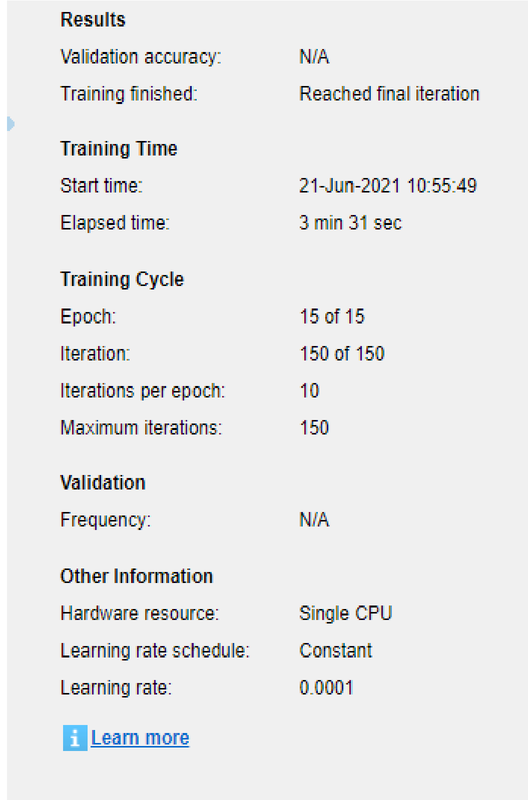

Figure 27 SqueezeNet results

4.8 LTSM Neural Network

After performing our experiment on MATLAB our final step is to use a recurrent neural network. This neural network is used for deep learning, and it has some feedback connections. It can process not only single data points (like photos), but also complete data sequences (such as speech or video). LSTM can be used for tasks like unsegmented, linked handwriting recognition, speech recognition, and anomaly detection in network traffic or IDSs, for example (intrusion detection systems).

Because there might be lags of undetermined duration between critical occurrences in a time series, LSTM networks are well-suited for categorizing, processing, and making predictions based on time series data. LSTMs were created to solve the problem of vanishing gradients that can occur when training traditional RNNs.

On this experiment it is inserted a layer which has only one sequence of data to be inputted. Bidirectional long-term dependencies between time steps of time series or sequence data are learned using a bidirectional LSTM (BiLSTM) layer. When you want the network to learn from the entire time series at each time step, these dependencies can be advantageous. This BiLTSM is set to 100 layers and output mode will be the name of the last output. The training data with 100 inputs which will also be cone and cylinder, will than train with properties of initial learn rate 0.01 seconds, doing it for 30 epochs. The training process is presented on figure 25.

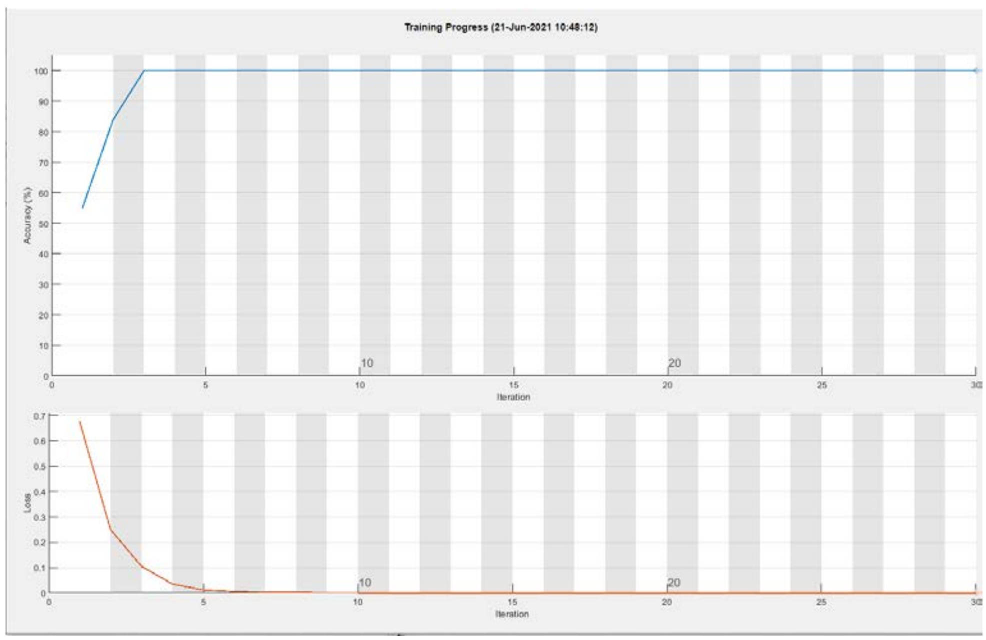

Figure 28 Training Process LTSM

On figure 28 we can see that the training process for LTSM was conducted in only 3 minutes and 36 seconds while training process for Resnet50 lasts 18 minutes. After training process with LTSM we also see the prediction of the training labels which have an accuracy of 100%. This is presented on figure 29.

Results	
Validation accuracy:	N/A
Training finished:	Reached final iteration
Training Time	
Start time:	21-Jun-2021 10:48:12
Elapsed time:	3 min 36 sec
Training Cycle	
Epoch:	30 of 30
Iteration:	30 of 30
Iterations per epoch:	1
Maximum iterations:	30
Validation	
Frequency:	N/A
Other Information	
Hardware resource:	Single CPU
Learning rate schedule:	Constant
Learning rate:	0.01

Figure 30 Results for LTSM training

```
predictedLabels = classify(RNNnet,testData,'ExecutionEnvironment','cpu');
accuracy = sum(predictedLabels == testLabels)/50*100
```

```
accuracy = 100
```

Figure 29 LTSM accuracy

4.9 MATLAB Experiment Conclusions

To conclude this section we would say that this example shows a procedure for utilizing machine and deep learning approaches to classify radar targets. Although this example uses simulated data for training and testing, it can simply be modified to work with real radar returns. Wavelet techniques were used for both the machine learning and CNN approaches due to signal properties. We were also able to achieve equivalent accuracy with this dataset by simply feeding the raw data into an LSTM. In more complex datasets, the raw data may be too fundamentally unpredictable for the model to learn robust features from the raw data, hence feature extraction may be required before utilizing an LSTM.

CHAPTER 5

CONCLUSIONS

This thesis has attempted to achieve a better understanding of radar classification and target detection by gathering different materials from various journals and books. Radar target detection and classification was surprisingly a very narrow field of research, all the journals and books which were related to this theme, have not reached any new accomplishment for almost 30 years.

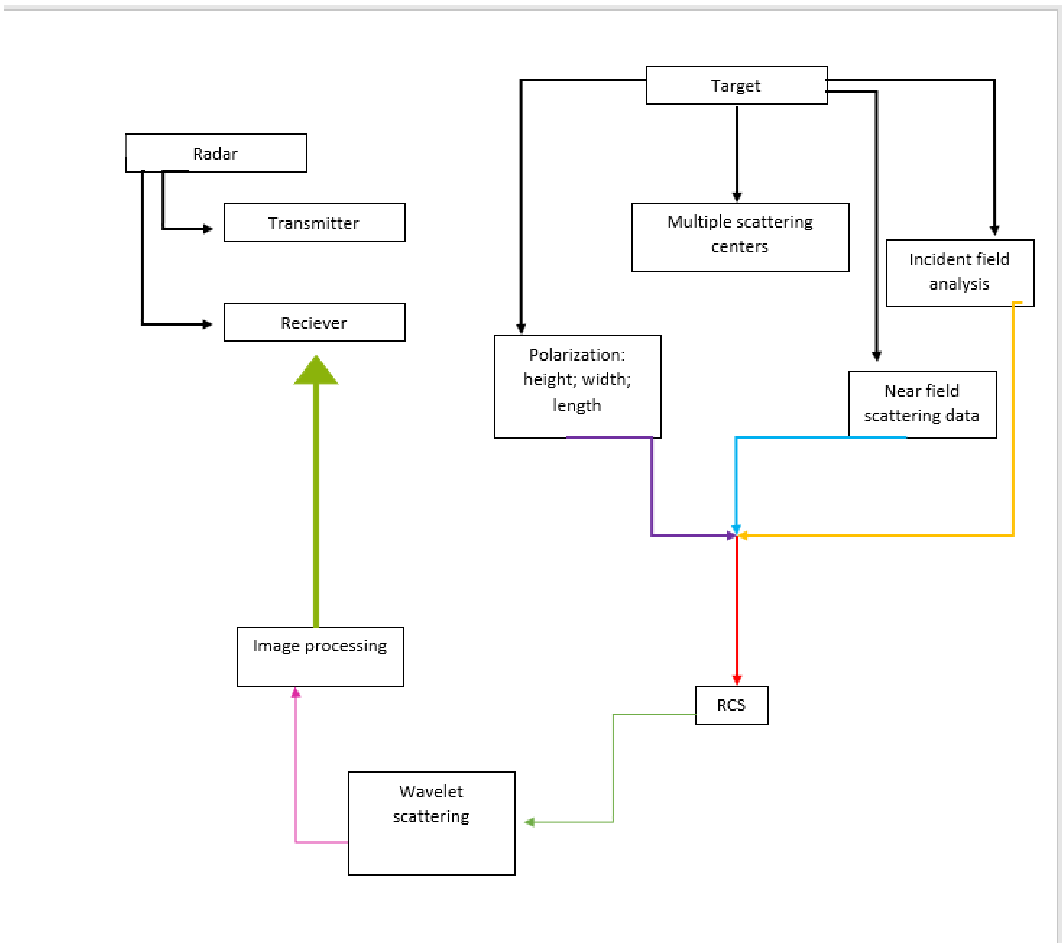

Figure 31 Summarized Image of Radar detection process.

Our thesis was organized in 5 chapters where the first and the second chapters provides a review for the introduction and literature that we used. Then we proceeded to give explanation of Radar Cross section and how this measurement of a radar’s capacity of scattering points, was able to give us a targets location. Target's RCS is determined by its aspect angle, frequency, and polarization. The impact of physical environment can be ignored. The RCS of a conducting plate with a physical region is considerably greater than the wavelength when the object dimension is significantly greater than the wavelength.

Using Wavelet transform and wavelet decomposition, we could easily detect a target. The scattering analysis of radar targets is done using four different time-frequency analysis approaches. The scattering mechanisms that characterize the behavior of objects in radar systems to incident waves can be divided into two types: dispersive and non-dispersive scattering mechanisms. Local scattering features can be retrieved from the local maxima of the target response in the time domain for non-dispersive scattering such as corners, edges, or specular reflections. In order to get the correct classification for a target we can use our prediction algorithm, which is explained step by step in chapter 4.

Our dissertation gives a new approach on radar target classification, by the experiment which was described on chapter 4. The study which we conducted gives a new perspective on target classification and reduction of time required to complete this process.

The experiment that we accomplished was by using simulated radar data, if this experiment was done using real data and statistics, we would have a better outcome, however this is to be seen in future work.

References

[1] Y. Bai, B. Hu and Z. Chen, "Targets dimension recognition based on RCS Wavelet pyramidal decomposition", *Proceedings of 2011 Cross Strait Quad-Regional Radio Science and Wireless Technology Conference*, 2011. Available: 10.1109/csqrwc.2011.6037150

[2] Thuong Le-Tien and Thong Dinh Nguyen, "A transformed image processing approach based on the continuous wavelet transform for non-dispersive scattering extraction", *TENCON '97 Brisbane - Australia. Proceedings of IEEE TENCON '97. IEEE Region 10 Annual Conference. Speech and Image Technologies for Computing and Telecommunications (Cat. No.97CH36162)*. Available: 10.1109/tencon.1997.647319

[3] "Matlab," Matlab, [Online]. Available: https://www.mathworks.com/help/radar/ug/radar-target-classification-using-machine-learning-and-deep-learning.html;jsessionid=ebdfcbc4555b932658ae2b52a053#d117e18632.

[4] C. Che Wan Fareez, O. Kama Azura, A. Nur Emileen and A. Noor Hafizah, "Forward Scattering Radar (FSR) ground target signal processing using wavelet technique (WT)", *2015 16th International Radar Symposium (IRS)*, 2015. Available: 10.1109/irs.2015.7226387

[5] S. Huang, W. Zhao and P. Luo, "Target Detection of SAR Image Based on Wavelet and Empirical Mode Decomposition", *2019 6th Asia-Pacific Conference on Synthetic Aperture Radar (APSAR)*, 2019. Available: 10.1109/apsar46974.2019.9048482

[6] Min Wang, Weimin Yuan and Shunjun Wu, "Impulse wave estimation based on analytic wavelet in UWB-radar", *Proceedings 7th International Conference on Signal Processing, 2004. Proceedings. ICSP '04. 2004.*. Available: 10.1109/icosp.2004.1442189

[7] Honghong Fan, Yingning Peng, Zhenming Feng, Xiuming Shan and Dajin Lu, "Interpreting scattering mechanism of radar target by wavelet transform", *Proceedings International Radar Conference*. Available: 10.1109/radar.1995.522583

[8] Z. Sebbani and G. Delisle, "RCS characterization using wavelet analysis", *11th International Symposium on Antenna Technology and Applied Electromagnetics [ANTEM 2005]*, 2005. Available: 10.1109/antem.2005.7852160

[9] G. Delisle, Z. Zebbani, C. Charrier and F. Cote, "A novel approach to complex target recognition using RCS wavelet decomposition", *IEEE Antennas and Propagation Magazine*, vol. 47, no. 1, pp. 35-55, 2005. Available: 10.1109/map.2005.1436218

[10] R. Abdullah, M. Rasid, M. Azis and M. Khalafalla, "Target prediction in Forward Scattering Radar", *2007 Asia-Pacific Conference on Applied Electromagnetics*, 2007. Available: 10.1109/apace.2007.4603914

[11] I. Choi and I. Rhee, "Performance Comparison of Time-Frequency Analysis Methods for Radar Signature Analysis", *2008 Second International Conference on Future Generation Communication and Networking*, 2008. Available: 10.1109/fgcn.2008.6

[12] D. Jamro, J. Hong, M. Bah and F. Mangi, "Novel triangular patch antenna with reduced radar cross section", *2014 11th International Computer Conference on Wavelet Actiev Media Technology and Information Processing(ICCWAMTIP)*, 2014. Available: 10.1109/iccwamtip.2014.7073428

[13] I. Jouny, "Wavelet decomposition of UWB radar signals", *IEEE Antennas and Propagation Society International Symposium 1992 Digest*, 1992. Available: 10.1109/aps.1992.221569

[14] N. Li, T. Zhang, X. Lv and S. Zhang, "An Improved Joint Time Frequency Approach for Shadow Image of Bistatic Forward Scattering Radar", *2006 CIE International Conference on Radar*, 2006. Available: 10.1109/icr.2006.343423

[15] F. Pereira, A. Vidal, V. Boria, A. Melcon and D. Rebenaque, "Radar Cross Section Computation of Multi-layered Dielectric and Magnetic Obstacles using an efficient Wavelet-like method", *2005 IEEE Antennas and Propagation Society International Symposium*. Available: 10.1109/aps.2005.1552183

[16] C. Charrier and G. Delisle, "Radar targets characterization using wavelets pyramidal decomposition", *1999 International Conference on Computational Electromagnetics and its Applications. Proceedings (ICCEA'99) (IEEE Cat. No.99EX374)*. Available: 10.1109/iccea.1999.825181

[17] Yuanqin Wang, Ruoyu Zhang, Jiacai Hong and Jing Sun, "Radar echo envelope extraction using Teager energy operator and wavelet transform", *APCCAS 2008 - 2008 IEEE Asia Pacific Conference on Circuits and Systems*, 2008. Available: 10.1109/apccas.2008.4746057

[18] H. Wilson and H. Leong, "An estimation and verification of vessel radar-cross-sections for HF surface wave radar", *2003 Proceedings of the International Conference on Radar (IEEE Cat. No.03EX695)*. Available: 10.1109/radar.2003.1278830

[19] R. Cariou, "Use of wavelets decomposition to reduce outside transmissions during measurement of RCS", *2010 International Conference on Electromagnetics in Advanced Applications*, 2010. Available: 10.1109/iceaa.2010.5650611

[20] M. Chen, X. Wu and W. Sha, "Fast frequency sweep analysis of RCS by accelerated asymptotic waveform evaluation method", *2010 3rd International Conference on Computer Science and Information Technology*, 2010. Available: 10.1109/iccsit.2010.5564010

[21] Youan Ke, "Invariant characters on radar cross section of polarized radar targets", *Record of the IEEE 2000 International Radar Conference [Cat. No. 00CH37037]*. Available: 10.1109/radar.2000.851906

[22] T. Jun and S. Ganlin, "Decomposition of Maneuvering Target RCS Based on Wavelet Analysis", *2010 First International Conference on Pervasive Computing, Signal Processing and Applications*, 2010. Available: 10.1109/pcspa.2010.240

[23] R. Mingqiu, C. Yichao, M. Liang and H. Yanfeng, "Complex signal envrionment analysis and cognition of multi-function radar", *2016 IEEE 9th UK-Europe-China Workshop on Millimetre Waves and Terahertz Technologies (UCMMT)*, 2016. Available: 10.1109/ucmmt.2016.7873982

[24] O. Bucci, L. Crocco, T. Isernia and V. Pascazio, "Wavelets in non-linear inverse scattering", IGARSS 2000. IEEE 2000 International Geoscience and Remote Sensing Symposium. Taking the Pulse of the Planet: The Role of Remote Sensing in Managing the Environment. Proceedings (Cat. No.00CH37120). Available: 10.1109/igarss.2000.860359

[25] Y.-W. Hsueh-JyhLi, The Electrical Engineering Handbook, Academic Press, 2005.

[26] H.-J. Li and Y.-W. Kiang, "Radar and Inverse Scattering," in The Electrical Engineering Handbook, Academic Press, 2005, pp. 671-690.

[27] T. Jun and S. Ganlin, "Decomposition of Maneuvering Target RCS Based on Wavelet Analysis", *2010 First International Conference on Pervasive Computing, Signal Processing and Applications*, 2010. Available: 10.1109/pcspa.2010.240

[28] A. Akansu, R. Haddad, P. Haddad and P. Haddad, Multiresolution Signal Decomposition: Transforms, Subbands, and Wavelets, 1st ed. Academic Press 2001, 2001, pp. 259-266.

[29] A. Almslmany, Recent advancements in airborne radar signal processing, 1st ed. IGI Global, pp. 120-180.

[30] J. Crispin and A. Maffett, "Radar cross-section estimation for simple shapes", Proceedings of the IEEE, vol. 53, no. 8, pp. 833-848, 1965. Available: 10.1109/proc.1965.4062

[31] D. Donald, Y. Everingham, L. McKinna and D. Coomans, "Feature Selection in the Wavelet Domain: Adaptive Wavelets", Comprehensive Chemometrics, pp. 647-679, 2009. Available: 10.1016/b978-044452701-1.00

[32] C. Che Wan Fareez, O. Kama Azura, A. Nur Emileen and A. Noor Hafizah, "Forward Scattering Radar (FSR) ground target signal processing using wavelet technique (WT)", *2015 16th International Radar Symposium (IRS)*, 2015. Available: 10.1109/irs.2015.7226387

[33] L. Wang, S. Dong, Z. Shang and S. Li, "Adaptive extended targets detection method based on wavelet transform in Gaussian clutter", *Proceedings of 2012 5th Global Symposium on Millimeter-Waves*, 2012. Available: 10.1109/gsmm.2012.6314096

[34] M. Ambrosanio, G. Schirinzi and V. Pascazio, "A mixed L2 — L1 norm minimization procedure for the data processing of ground penetrating radar", *2017 IEEE International Geoscience and Remote Sensing Symposium (IGARSS)*, 2017. Available: 10.1109/igarss.2017.8127814

[35] W. Jiang, W. Li, Y. Huang, Z. Liu, J. Wu and J. Yang, "Radar angular superresolution algorithm based on Fourier-Wavelet regularized deconvolution", *2013 IEEE International Geoscience and Remote Sensing Symposium - IGARSS*, 2013. Available: 10.1109/igarss.2013.6723114

[36] Chen Guoying and Huang Peikang, "Monopulse radar angle measurement error reduction based on wavelet multiresolution analysis", *Proceedings of International Radar Conference*. Available: 10.1109/icr.1996.574593

[37] Luo Hong, Xu Xiaojian and Huang Peikang, "Prediction and representation for wideband signatures of radar targets", Proceedings of International Radar Conference. Available: 10.1109/icr.1996.574575

[38] C. Charrier and G. Delisle, "Radar targets characterization using wavelets pyramidal decomposition", 1999 International Conference on Computational Electromagnetics and its Applications. Proceedings (ICCEA'99) (IEEE Cat. No.99EX374). Available: 10.1109/iccea.1999.825181

[39] He Guanghui, Shen Xiuming, Fen Zhenming, Fan Honghong, Peng Yinnin and Lu Dajing, "Study of two methods in radar target recognition", Proceedings of International Radar Conference. Available: 10.1109/icr.1996.574574

[40] Tse-Tong Chia and Zhonggui Xiang, "A hybrid technique for analysis of scattering from circular cavities with cylindrically periodic terminations", IEEE Antennas and Propagation Society International Symposium. Transmitting Waves of Progress to the Next Millennium. 2000 Digest. Held in conjunction with: USNC/URSI National Radio Science Meeting (Cat. No.00CH37118). Available: 10.1109/aps.2000.874604

[41] Hai Deng and Hao Ling, "Efficient representation of electromagnetic integral equations using pre-defined wavelet packet basis", IEEE Antennas and Propagation Society International Symposium. 1999 Digest. Held in conjunction with: USNC/URSI National Radio Science Meeting (Cat. No.99CH37010). Available: 10.1109/aps.1999.789148

[42] R. Mingqiu, C. Yichao, M. Liang and H. Yanfeng, "Complex signal envrionment analysis and cognition of multi-function radar", 2016 IEEE 9th UK-Europe-China Workshop on Millimetre Waves and Terahertz Technologies (UCMMT), 2016. Available: 10.1109/ucmmt.2016.7873982

[43] Y. Ruan and S. Deng, "RCS analysis of reflector antennas by complex ray expansion", International Symposium on Antennas and Propagation Society, Merging Technologies for the 90's, 1990. Available: 10.1109/aps.1990.115467

[44] C. Spooner, M. Clark and L. McWhorter, "Wavelet-based compression of HRR radar data for moving targets", Conference Record of the Thirty-Fourth Asilomar

Conference on Signals, Systems and Computers (Cat. No.00CH37154). Available: 10.1109/acssc.2000.911245

[45] Guangwen Pan, "Wavelets: a promising approach to linear and nonlinear modeling of electromagnetic problems", ICMMT'98. 1998 International Conference on Microwave and Millimeter Wave Technology. Proceedings (Cat. No.98EX106). Available: 10.1109/icmmt.1998.768218

[46] Yuanqin Wang, Ruoyu Zhang, Jiacai Hong and Jing Sun, "Radar echo envelope extraction using Teager energy operator and wavelet transform", APCCAS 2008 - 2008 IEEE Asia Pacific Conference on Circuits and Systems, 2008. Available: 10.1109/apccas.2008.4746057

[47] M. Williams and A. Beex, "Radar cross-section data encoding based on AR spectral estimation techniques", Proceedings International Radar Conference. Available: 10.1109/radar.1995.522541

[48] He Guanghui, Shen Xiuming, Fen Zhenming, Fan Honghong, Peng Yinnin and Lu Dajing, "Study of two methods in radar target recognition", Proceedings of International Radar Conference. Available: 10.1109/icr.1996.574574

[49] Min-Chin Lin, Yean-Woei Kiang and Hsueh-Jyh Li, "Experimental discrimination of wire stick targets using multiple-frequency amplitude returns", *IEEE Transactions on Antennas and Propagation*, vol. 40, no. 9, pp. 1036-1040, 1992. Available: 10.1109/8.166528

[50] I. Jouny, "Scattering centers extraction using EWT for target identification", *2016 IEEE Conference on Antenna Measurements & Applications (CAMA)*, 2016. Available: 10.1109/cama.2016.7815735

[51] A. Akansu, "Wavelets and filter banks. A signal processing perspective", *IEEE Circuits and Devices Magazine*, vol. 10, no. 6, pp. 14-18, 1994. Available: 10.1109/101.329928